Received: 31 March 2020 | Revised: 8 June 2020 | Accepted: 23 June 2020

DOI: 10.1096/fj.202000754R

RESEARCH ARTICLE

THE FASEB JOURNAL

Depletion of cyclic-GMP levels and inhibition of cGMP-dependent protein kinase activate $p21^{Cip1}/p27^{Kip1}$ pathways and lead to renal fibrosis and dysfunction

Subhankar Das | Kandasamy Neelamegam | Whitney N. Peters | Ramu Periyasamy | Kailash N. Pandey

Department of Physiology, Tulane University Health Sciences Center, School of Medicine, New Orleans, LA, USA

Correspondence
Kailash N. Pandey, Department of Physiology, Tulane University Health Sciences Center, School of Medicine, 1430 Tulane Avenue, New Orleans, LA 70112, USA.
Email: kpandey@tulane.edu

Funding information
HHS | NIH | National Heart, Lung, and Blood Institute (NHLBI), Grant/Award Number: HL062147

Abstract

Cell-cycle regulatory proteins ($p21^{Cip1}/p27^{Kip1}$) inhibit cyclin and cyclin-dependent kinase (CDK) complex that promotes fibrosis and hypertrophy. The present study examined the role of CDK blockers, $p21^{Cip1}/p27^{Kip1}$ in the progression of renal fibrosis and dysfunction using *Npr1* (encoding guanylyl cyclase/natriuretic peptide receptor-A, GC-A/NPRA) gene-knockout (0-copy; $Npr1^{-/-}$), 2-copy ($Npr1^{+/+}$), and 4-copy ($Npr1^{++/++}$) mice treated with GC inhibitor, A71915 and cGMP-dependent protein kinase (cGK) inhibitor, (Rp-8-Br-cGMPS). A significant decrease in renal cGMP levels and cGK activity was observed in 0-copy mice and A71915- and Rp-treated 2-copy and 4-copy mice compared with controls. An increased phosphorylation of Erk1/2, p38, $p21^{Cip1}$, and $p27^{Kip1}$ occurred in 0-copy and A71915-treated 2-copy and 4-copy mice, while Rp treatment caused minimal changes than controls. Pro-inflammatory (TNF-α, IL-6) and pro-fibrotic (TGF-β1) cytokines were significantly increased in plasma and kidneys of 0-copy and A71915-treated 2-copy mice, but to lesser extent in 4-copy mice. Progressive renal pathologies, including fibrosis, mesangial matrix expansion, and tubular hypertrophy were observed in 0-copy and A71915-treated 2-copy and 4-copy mice, but minimally occurred in Rp-treated mice compared with controls. These results indicate that *Npr1* has pivotal roles in inhibiting renal fibrosis and hypertrophy and exerts protective effects involving cGMP/cGK axis by repressing CDK blockers $p21^{Cip1}$ and $p27^{Kip1}$.

KEYWORDS
CDK blockers, cGMP/cGK, gene-targeting, natriuretic peptides, NPRA, renal fibrosis

Abbreviations: Alb:Cr, albumin:creatinine; CDK, cyclin-dependent kinase; cGKs, cGMP-dependent protein kinases; cGK inhibitor, Rp-8-Br-cGMPS; cGK I, cGMP-dependent protein kinase I; cGK II, cGMP-dependent protein kinase II; DTT, dithiothreitol; ECL, enhanced chemiluminescence; Erk1/2, extracellular-regulated kinase 1/2; GAPDH, glyceraldehyde-3-phosphate dehydrogenase; GC-A/NPRA, Guanylyl cyclase/natriuretic peptide receptor-A; H&E, hematoxylin and eosin; IL-6, interleukin-6; KC, kidney collagen; KW, kidney weight; MAPKs, mitogen-activated protein kinases; MCs, mesangial cells; MKP-1, MAPK phosphatase-1; MME, mesangial matrix expansion; NO, nitric oxide; *Npr1*, encoding GC-A/NPRA; $p21^{Cip1}$, CDK interacting protein 1; $p27^{Kip1}$, kinase inhibitory protein 1; PBST, phosphate-buffered saline-Tween 20; PCNA, proliferating cell nuclear antigen; PCR, polymerase chain reaction; PVDF, polyvinyl difluoride; SBP, systolic blood pressure; SDS, sodium dodecyl sulfate; TBST, Tris-buffered saline-Tween 20; TGF-β1, transforming growth factor-beta 1; TNF-α, tumor necrosis factor-alpha; VSMCs, vascular smooth muscle cells.

1 | INTRODUCTION

Interaction of atrial and brain natriuretic peptides (ANP and BNP) with guanylyl cyclase/natriuretic peptide receptor-A (GC-A/NPRA) has a central role in the pathophysiology of hypertension, renal disorders, and cardiovascular dysfunction.[1-4] Mice carrying targeted global disruption of the *Npr1* gene (encoding for GC-A/NPRA) exhibit hypertension, kidney dysfunction, and congestive heart failure.[5-9] GC-A/NPRA antagonizes renal hypertrophic and fibrotic growth, thus conferring renoprotective effects in disease states.[10-13] Global deletion of *Npr1* from mice led to increased tubular hypertrophy and enhanced mesangial matrix expansion (MME) with subsequent development of fibrosis in the kidneys.[10,11,13-15] GC-A/NPRA-mediated synthesis and intracellular accumulation of cGMP, as well as subsequent activation of cGMP-dependent protein kinases (cGKs), elicit a wide range of effects under both physiological and pathophysiological conditions.[16-20] cGKs are expressed in a wide range of tissues and cell types, including intra- and extra-glomerular cells, mesangial cells (MCs), vascular smooth muscle cells (VSMCs), and interstitial myofibroblasts.[20-22] It has been shown that increasing cGK activity protects mice against acute renal injury and fibrosis in an ischemia-reperfusion-induced kidney injury animal model.[19,23-25] Increased cGK activity has been found to inhibit high-glucose-induced thrombospondin 1-dependent extracellular matrix accumulation in the kidneys, suggesting that cGK has an anti-fibrotic effect in chronic kidney diseases.[26,27] Treatment with GC activators, including natriuretic peptides or nitric oxide (NO) donor, suppressed renal fibrosis via cGK I pathways.[24] However, the underlying mechanism by which this occurs is still unknown.

Several studies have shown that cells in arrest in the G1 phase of the cell cycle undergo hypertrophy, supporting the idea that the cell cycle plays a critical role in renal disease states.[28-30] It has been shown that in hypertrophic and fibrotic disease conditions, agonist-induced G1 arrest is associated with upregulation of the cyclin-dependent kinase (CDK) inhibitors, $p21^{Cip1}$ (cDK interacting protein 1) and $p27^{Kip1}$ (kinase inhibitory protein 1).[31-34] Expression of CDK-inhibitors ($p21^{Cip1}$ and $p27^{Kip1}$) is increased by high glucose in mesangial cells in vivo and in vitro.[35-38] The CDK inhibitors are regulated by the activation of mitogen-activated protein kinases (MAPKs), which varies with cell types, stimuli, and the duration of signal activation. In fibroblasts, MAPK activation leads to increased $p27^{Kip1}$ degradation that is independent of phosphorylation by CDK2/cyclin E.[39-41] In contrast, more delayed and prolonged activation of MAPKs in PC12 cells and fibroblasts by nerve growth factor leads to cell-cycle arrest, which is associated with extracellular-regulated kinase 1/2 (Erk1/2)-dependent increases in the expression of $p27^{Kip1}$.[42]

The constitutive expression of MAPK phosphatase-1 (MKP-1) has been found to attenuate serum or oncogenic *ras*-induced MAPKs activation, block MAPK-dependent gene expression, and inhibit cell proliferation, suggesting that the dephosphorylation of MAPKs in vivo by MKP-1 could have a negative effect on cell proliferation and hypertrophy.[43-46] Earlier, we reported that ANP/NPRA/cGMP signaling inhibits MAPKs in MCs and VSMCs; however, it also stimulates MKP-1 in these cells.[47,48] Previously, we also demonstrated that systemic deletion of GC-A/NPRA produced renal mesangial cell expansion and hypertrophy in *Npr1* gene-knockout mice.[10,11] In the present study, we hypothesized that the anti-proliferative, anti-hypertrophic, and anti-fibrotic actions of GC-A/NPRA might be mediated through the cGMP/cGK axis by induction of MKP-1, which dephosphorylates Erk/p38/$p21^{Cip1}$/$p27^{Kip1}$ and induces G_0/G_1 cell-cycle transition to control the fibrosis and hypertrophy. To test this hypothesis, we examined the effect of *Npr1* ablation and drug treatments of wild-type and gene-duplicated *Npr1* mice with cGK inhibitor, Rp-8-Br-cGMPS (Rp) and NPRA antagonist, A71915. Furthermore, we determined the expression and the activation of CDK-inhibitors, $p21^{Cip1}$ and $p27^{Kip1}$ and their physiological effects on the kidney injury and disorders in both genetically modified and drug-treated animals.

2 | MATERIALS AND METHODS

2.1 | Materials

Primary antibodies of cGMP-dependent protein kinase 1 (cGK I), cGK II, proliferating cell nuclear antigen (PCNA), MAPK phosphatase-1 (MKP-1), p-Erk1/2, p-p38, $p21^{Cip1}$, and $p27^{Kip1}$ were obtained from Santa Cruz Biotechnology (San Diego, CA, USA). Anti-mouse secondary antibody conjugated with Alexa Fluor 647, 488 and ProLong Gold antifade reagent with 4′, 6-diamidino-2-phenylindole (DAPI) were purchased from Molecular Probes (Invitrogen, Eugene, OR, USA). A71915 and Rp-8-Br-cGMPS (hereafter indicated as Rp) were purchased, respectively, from Bachem (Torrance, CA, USA) and EMD Calbiochem (San Diego, CA, USA). TRIzol reagent was obtained from Invitrogen (Carlsbad, CA, USA). A creatinine kit was purchased from BioAssay System (Hayward, CA, USA). A microalbumin assay kit was purchased from Bethyl Laboratories (Montgomery, TX, USA). RNase-free DNase was obtained from Qiagen (Valencia, CA, USA). A multiplex kit for mouse cytokine assay was purchased from Millipore (Billerica, MA, USA). A cGK activity assay kit was purchased from MBL International (Woburn, MA, USA). A cGMP assay kit was purchased from Assay Designs (Ann Arbor, MI, USA). All other chemicals were of reagent grade.

2.2 | Generation of *Npr1* gene-knockout and gene-duplicated mice

Gene-targeted (gene-knockout and gene-duplication) *Npr1* mice were generated by homologous recombination as previously reported.[1,49] Briefly, gene-disruption targeting vector was constructed using both a 6.5-kb fragment of strain 129 genomic DNA containing sequence upstream of the 5′ *Npr1* coding region as the 5′ region of homology and a 1.5-kb fragment containing exon 2, intron 2, and part of exon 3 as the 3′ homology arm. Animals were made from correctly targeted embryonic stem (ES) cells.[50] Similarly, the targeted gene-duplication of *Npr1* was achieved by homologous recombination.[51] Briefly, the duplication targeting construct was made by inserting the same 6.5-kb fragment in opposite orientations in the targeting vector and replacing the 1.5-kb fragment with a 1.3-kb Hind III fragment containing sequence 6.0-kb downstream of the last *Npr1* encoding exon.[51] All mice were littermate progenies of C57/BL6 genetic background. The animals were genotyped by polymerase chain reaction (PCR) analyses of DNA isolated from tail biopsies as previously reported.[49,52] Mice were bred and maintained in the Animal Care Facility at Tulane University Health Sciences Center. All animal procedures were followed under protocols approved by the Institutional Animal Care and Use Committee and conducted in compliance with the National Institutes of Health (NIH) Guide for the Care and Use of Laboratory Animals. The genotypes of mice included 0-copy (−/−) homozygous null mutant mice, 2-copy (+/+) wild-type mice, and 4-copy (++/++) homozygous gene-duplicated mice. Animals were maintained in a 12:12 hours light-dark cycle (6 AM to 6 PM) at 25°C and fed regular chow (Purina Laboratory, St. Louis, MO, USA) and tap water ad libitum.

2.3 | Experimental animals

We used adult (12-16 weeks) male 0-copy, 2-copy, and 4-copy littermate mice. There were seven groups of animals: (a) 0-copy, sham; (b) 2-copy, sham; (c) 2-copy + A71915 (1 μg/ kg/day); (d) 2-copy + Rp-8-Br-cGMPS (5 μg/kg/day); (e) 4-copy, sham; (f) 4-copy + A71915 (1 μg/kg/day); and (g) 4-copy + Rp-8-Br-cGMPS (5 μg/kg/day). Eight to 10 mice were used in each group. All drugs were subcutaneously infused for 15 days using an osmotic minipump (Alzet Durect, Cupertino, CA, USA).

2.4 | Blood pressure analysis

The arterial systolic blood pressure (SBP) of *Npr1* mice was measured every other day by the noninvasive computerized tail-cuff method, using a Visitech BP2000.[10,53] After 7 days of training the mice for arterial pressure measurement, an average SBP level of five sessions per day was calculated for analysis.

2.5 | Blood and tissue collection

With mice under CO_2 anesthesia, blood was collected by cardiac puncture in prechilled tubes containing 10 μL of heparin (1000 USP units/mL). Plasma was separated by centrifugation at 3000 *g* for 10 minutes at 4°C and stored at −80°C until use. Animals were euthanized by administration of a high concentration of CO_2 gas. Kidney tissues were collected, flash-frozen in liquid nitrogen, and stored at −80°C until use.

2.6 | Renal histopathology and morphological studies

Kidney tissues from each group were fixed in 10% buffered paraformaldehyde solution. Paraffin-embedded tissue sections (5-μm) were stained with hematoxylin and eosin (H&E) and with Masson's trichrome to assess the presence of interstitial collagen fiber accumulation as a marker of renal fibrosis. The percentage of matrix mesangial expansion (MME), tubular hypertrophy, tubulointerstitial nephritis, and perivascular infiltration (monocyte/macrophage) relative to the total kidney area was determined in blinded and unbiased manner by analysis in 20 randomly selected microscopic fields in 6-8 kidney sections per animal, using ImagePro Plus image analysis software (Media Cybernetics, Silver Spring, MD) as earlier reported.[5,10] The ratio of fibrosis to total kidney was determined by visualizing the blue-stained areas in blinded and unbiased manner as previously reported.[10]

2.7 | Analysis of gene expression by real-time qRT-PCR

Total RNA was isolated using the TRIZOL method. Kidney tissues (30 mg) were homogenized and the RNA was extracted as per manufacturer's instructions. The purified RNA for each sample was used for quantitative real-time PCR (qRT-PCR). First-strand cDNA was synthesized from 1 μg of total RNA in a final volume of 20 μL using RT^2 First Strand kit (Qiagen, Valencia, CA, USA). qRT-PCR was performed using the Mx3000P real-time PCR system and data were analyzed with MxPro software (Stratagene, La Jolla, CA, USA) as previously described.[10,54] The forward (F) and reverse (R) primers used were: TNF-α, F-5′-caacgccctcctggccaacg-3′ and R-5′-tcggggcagccttgtccctt-3′; IL-6, F-5′-cacggcctt ccctacttcac-3′ and R-5′-tgcaagtgcatcatcgttgt-3′; TGF-β1,

F-5′-tacagggctttcgattcagc-3′ and R-5′-gtga gctgtgcaggt gct-3′; cGK I, F-5′-ctgcctctcctctccttcct-3′ and R-5′-tcgcaaa gtcttcctccagt-3′; cGK II, F-5′-agtgcctctggatgttcacc-3′ and R-5′-ctggggatccaatctcttca-3′; and GAPDH, F-5′-tccctcaagattgtcagcaa-3′ and R-5′-agatccacaaacggatacatt-3′. PCR amplification (triplicates) was carried out in a 20 µL reaction volume using RT^2 real-time quantifast SYBR Green/ROX PCR Master Mix. The PCR reaction conditions were: 95°C for 10 minutes; followed by 45 cycles at 95°C for 15 seconds and 60°C for 1 minutes; followed by 1 cycle at 95°C for 1 minutes, 55°C for 30 seconds and 95°C for 30 seconds for the dissociation curve. The reaction mixture without template cDNA was used as negative controls. Threshold cycle numbers (C_T) were determined with MxPro QPCR Software and transformed using the ΔC_T comparative method. The quantitative fold changes in mRNA expression were normalized to expression values of GAPDH mRNA as endogenous control within each corresponding sample relative to positive and negative controls. The levels of gene expression in each corresponding group were determined by the comparative C_T method ($\Delta\Delta C_T$) using REST2009 software from Qiagen (Valencia, CA, USA). After PCR amplification, a melting curve of each amplicon was determined to verify its accuracy.

2.8 | Western blot analysis

Kidney tissue homogenate (20 µg proteins) was mixed with an equal volume of 2X sodium dodecyl sulfate (SDS) sample loading buffer containing 125 mM Tris-HCl, 4% SDS, 20% glycerol, 100 mM dithiothreitol (DTT), and 0.2% bromophenol blue, then separated in a 10% SDS-polyacrylamide gel as previously described.[5,54] Proteins were electrotransferred onto a polyvinyl difluoride (PVDF) membrane. The membrane was blocked with 1X Tris-buffered saline-Tween 20 (TBST; 25 mM Tris, 500 mM NaCl, and 0.05% Tween 20, pH 7.5) containing 5% fat-free milk, then incubated overnight in TBST containing 3% fat-free milk at 4°C with primary antibodies as previously described.[5,10] The membrane was then treated with corresponding secondary HRP-conjugated antibodies (1:5000 dilution). Protein bands were visualized by enhanced chemiluminescence (ECL) plus detection system with an Alpha Innotech Imager. In the Western blotting, primary antibodies were used as follows: cGK I (75 kDa; sc-271766; 1:500; SCBT, Santa Cruz, CA, USA); cGK II (86 kDa; sc-393126; 1:500); MKP-1 (40 kDa; sc-373841; 1:200; SCBT, Santa Cruz, CA, USA); Erk1/2 (44 kDa/42 kDa; sc-514302; 1:250; SCBT, Santa Cruz, CA, USA); p38 (38 kDa; sc-271120; 1:250; SCBT, Santa Cruz, CA, USA); p-Erk1/2 (44 kDa/42 kDa; sc-81492; 1:200; SCBT, Santa Cruz, CA, USA); p-p38 (38 kDa; sc-7973; 1:250; SCBT, Santa Cruz, CA, USA); $p21^{Cip1}$ (21 kDa; sc-6246; 1:250; SCBT, Santa Cruz, CA, USA); $p27^{kip1}$ (27 kDa;sc-1641; 1:200; SCBT, Santa Cruz, CA, USA); β-actin (43 kDa; sc-47778; 1:2000; SCBT, Santa Cruz, CA, USA); PCNA (36 kDa; sc-56; 1:500; SCBT, Santa Cruz, CA, USA); HRP-conjugated anti mouse IgG (sc-516102; 1:1000; SCBT, Santa Cruz, CA, USA; G-21040; 1:1000; Invitrogen, Eugene, OR, USA).

2.9 | Assay of albumin and creatinine in urine samples

Albumin levels were measured in 24-hours urine samples collected from mice in a metabolic cage, using ELISA kit (Bethyl Laboratories, Montgomery, TX, USA). Urine creatinine concentrations were measured using the creatinine assay kit (BioAssay Systems, Hayward, CA, USA).[10,55]

2.10 | Determination of collagen concentrations in kidney tissues

Total collagen concentrations in kidney tissue samples were quantified from the hydroxyproline content as previously described.[56] Briefly, the tissue samples were homogenized and hydrolyzed in 6 N HCl at 110°C for 18 hours in a sealed reaction vial. The samples were dried under vacuum and the residue was resuspended in 50% isopropanol, then treated with chloramine T. After 10 minutes of incubation, the samples were mixed with Ehrlich's reagent and incubated at 50°C for 90 minutes. The absorbance was read at 558 nm using water as a reference; readings were corrected with a reagent blank. To obtain the total collagen content, a conversion factor of 8.2 was used.

2.11 | Assay of plasma and renal pro-inflammatory cytokines

The concentrations of pro-inflammatory and pro-fibrotic cytokines, including tumor necrosis factor-alpha (TNF-α), interleukin-6 (IL-6), and transforming growth factor-beta1 (TGF-β1), were measured in plasma and kidney tissue homogenates by multiplex bead array format (Milliplex and Lincoplex) from Millipore (Billerica, MA, USA), using a Bio-Plex Instrument (Bio-Rad, Hercules, CA, USA) according to the manufacturer's guidelines. Spectrally addressed polystyrene beads coated with cytokine-specific monoclonal antibodies were used to capture the cytokine of interest. The instrument sorted out and measured the fluorescent signal from each bead by dual excitation sources.

2.12 | Immunofluorescence analysis

Immunofluorescence staining was done on 4-μm sections of paraffin-embedded kidney tissues. After dehydration and antigen retrieval, the sections were sequentially incubated at room temperature with blocking reagent, primary antibodies (PCNA, $p21^{Cip1}$, $p27^{Kip1}$, cGK I, cGK II) and secondary antibody conjugated with respective fluorochrome for 30 minutes.[5,57] The sections were then washed with phosphate-buffered saline-Tween 20 (PBST), after which an appropriate amount of ProLong-Gold Antifade reagent with DAPI was added. The nonspecific binding of secondary antibodies was excluded by omitting the primary antibody. The specificity of the primary antibody was tested using the PBS solution without antibody; this served as a control. Immunofluorescence was observed and photographed under a fluorescence microscope (Olympus BX51) with integrated Magnafire Digital Firewire Camera Software. The antibody-positive area relative to the area of the total kidney was calculated using ImagePro Plus image analysis software (Media Cybernetics, Silver Spring, MD, USA).

2.13 | Plasma and kidney cGMP assay

Blood samples were collected in tubes containing EDTA and immediately centrifuged at 3000 *g* for 10 minutes at 4°C. The plasma was separated and stored at −80°C until used. Kidney tissues were also collected simultaneously, and flash frozen in liquid nitrogen, and immediately stored at −80°C until use. Plasma and renal cGMP levels were determined using a direct cGMP enzyme-linked immunoassay kit (Assay Designs, Ann Arbor, MI, USA), according to the manufacturer's protocol as previously reported.[8,10]

2.14 | Renal cGK activity assay

Renal cGK activity was determined in *Npr1* 0-copy, 2-copy, and 4-copy mice with and without treatment of cGK inhibitor, Rp-8-Br-cGMPS (5 μg/kg/day), and NPRA antagonist, A71915 (1 μg/kg/day). Nuclear fraction from the kidney was prepared and subjected to cGK activity assay using the CycLex cGMP-dependent protein kinase assay kit (MBL International, Woburn, MA, USA) according to the manufacturer's protocols. The CycLex cGK assay uses a peroxidase coupled anti-phospho-G kinase substrate monoclonal antibody reporter molecule. The assay system provides a non-radioactive, sensitive, and specific method to measure the cGK activity.[58]

2.15 | Statistical analysis

Statistical analysis was done by one-way analysis of variance (ANOVA and nonparametric) with Dunnett's multiple comparison post hoc tests, using the GraphPad PRISM program (version 6.0; GraphPad Software, San Diego, CA). The results are presented as mean ± SE. Significance was set at $P < .05$.

3 | RESULTS

3.1 | Renal analytical and functional measurements

The SBP, kidney weight (KW), and urine albumin:creatinine (Alb:Cr) ratios were determined in all experimental groups (Table 1). BP analysis showed a high SBP in 0-copy mice (138.6 ± 3.3 mm Hg; $P < .001$) and a significantly lower SBP in 4-copy mice (86.0 ± 2.8 mm Hg; $P < .01$) as compared to 2-copy control animals (102.2 ± 1.7 mm Hg). Moreover, treatment with A71915 and Rp for 15 days showed significant changes in SBP in 2-copy mice but A71915 treatment caused only a small but significant increase in SBP of 4-copy mice as compared with untreated control mice (Table 1). There was a marked increase in KW of 0-copy mice (256.8 ± 2.7 mg; $P < .001$) as compared with 2-copy wild-type mice (231.0 ± 2.1 mg) and 4-copy gene-duplicated mice (222.6 ± 1.8). After A71915 treatment there was a significant increase in KW of 2-copy (239.2 ± 1.9 mg; $P < .05$) mice, but no significant change was observed in the KW of Rp-treated 2-copy mice (233.6 ± 1.9 mg). Similarly, treatment with NPRA inhibitor, A71915 also did not cause significant change in KW in 4-copy mice as compared with untreated control mice (Table 1). On the other hand, the Alb:Cr ratio was significantly increased in 0-copy mice (three-fold) when compared with 2-copy mice (5.4 ± 0.2 vs 1.6 ± 0.1; $P < .001$). While A71915 treatment showed a significant increase (75%) in Alb:Cr in 2-copy mice (2.8 ± 0.1), this value remained unchanged in the Rp-treated group. Furthermore, after 15 days of treatment, both inhibitors showed only minimal changes in Alb:Cr in 4-copy animals as compared to 2-copy wild-type mice (Table 1).

3.2 | Quantitation of collagen and cGMP contents

The kidney collagen (KC) and renal cGMP contents were determined in all the experimental groups (Table 1). KC content was significantly increased (two-fold) in 2-copy mice treated with A71915 (2.3 ± 0.3 μg/gm), but was unchanged in the Rp-treated group (1.3 ± 0.2 μg/gm) as compared with 2-copy untreated control mice (1.1 ± 0.1 μg/gm). Similar increases (three-fold) in KC contents were observed in 0-copy mice (3.3 ± 0.3 μg/gm). KC content was increased in 4-copy + A71915 mice but was unchanged in Rp-treated 4-copy mice compared with 4-copy untreated control mice.

TABLE 1 Analyses of systolic blood pressure, urine albumin/creatinine, kidney collagen, renal cGMP in *Npr1* gene-disrupted, wild-type and gene-duplicated mice with or without treatments of Rp-8-Br-cGMPS (Rp) and A71915 for 15 days

			2-copy			4-copy	
Parameters	**0-copy**	**2-copy**	**Rp**	**A71915**	**4-copy**	**Rp**	**A71915**
SBP (mm Hg)	138.6 ± 3.3[§]	102.2 ± 1.7	110.8 ± 1.2[€]	115.0 ± 1.5[b]	86.0 ± 2.8	91.0 ± 2.0	95.4 ± 1.9[#]
KW (mg)	256.8 ± 2.7[§]	231.0 ± 2.1	233.6 ± 1.9	239.2 ± 1.9[a]	222.6 ± 1.8	226.0 ± 2.2	225.6 ± 2.8
Alb:Cr (Urine)	5.4 ± 0.2[§]	1.6 ± 0.1	1.9 ± 0.2	2.8 ± 0.1[b]	1.5 ± 0.1	1.7 ± 0.1	1.8 ± 0.1
KC (μg/gm)	3.3 ± 0.3[§]	1.1 ± 0.1	1.3 ± 0.2	2.3 ± 0.3[b]	0.9 ± 0.1	1.0 ± 0.1	1.2 ± 0.1
Renal cGMP (pmole/mg pr)	5.8 ± 0.7	36.8 ± 2.2	29.5 ± 1.7[€]	15.5 ± 2.1[c]	74.4 ± 4.0	68.1 ± 3.1	60.8 ± 2.8[#]
Plasma cGMP (pmole/mL)	2.5 ± 0.4[§]	19.1 ± 1.1	14.9 ± 1.5[€]	7.4 ± 0.7[c]	40.9 ± 2.5	34.6 ± 2.5	29.9 ± 2.0[#]

Note: Systolic blood pressure (SBP) was measured by computerized tail-cuff method. The urine albumin, creatinine, kidney collagen, albumin and creatinine ratio, and cGMP levels were determined as described under Materials and Methods section. The data are expressed as mean ± SE. n = 8 in each group.

[a]$P < .05$ (untreated 2-copy vs A71915-treated wild-type, 2-copy).

[b]$P < .01$ (untreated 2-copy vs A71915-treated wild-type, 2-copy).

[c]$P < .001$ (untreated 2-copy vs A71915-treated wild-type, 2-copy).

[€]$P < .05$ (untreated 2-copy vs Rp-treated wild-type, 2-copy).

[#]$P < .05$ (untreated gene-duplicated 4-copy vs A71915-treated gene-duplicated, 4-copy).

[§]$P < .0001$ (untreated 0-copy vs untreated wild-type, 2-copy).

The treatments of 2-copy mice with Rp and A71915 showed a significant reduction in kidney cGMP content (29.5 ± 1.7 and 15.5 ± 2.1 pmole/mg protein) as compared to that of control 2-copy mice (36.8 ± 2.2 pmole/mg protein). Treatment with A71915 led to a significant reduction in renal cGMP content in 4-copy mice (60.8 ± 2.8 pmole/mg protein; $P < .05$), while Rp treatment produced only a modest change in renal cGMP content in 4-copy mice (Table 1). Similarly, we found a significant reduction in plasma cGMP levels in 0-copy mice (2.5 ± 0.4 pmole/mL; $P < .001$), a proportionate significant increase (two-fold) in plasma cGMP concentration occurred in untreated 4-copy mice (40.9 ± 2.5 pmole/mL; $P < .001$) as compared to 2-copy mice (19.1 ± 1.1 pmole/mL). Plasma cGMP content was significantly reduced in 2-copy mice after treatment with both A71915 (7.4 ± 0.7 pmole/mL; $P < .001$) and Rp (14.9 ± 1.5 pmole/mL; $P < .05$).

3.3 | Renal cGK activity and cGK expression

The results of renal cGK activity assays are shown in Figure 1. The endogenous cGK activity in kidney tissues was downregulated in 0-copy mice by 60% ($P < .001$), in 2-copy + A71915 mice by 53% ($P < .01$), and in 2-copy + Rp mice by 39% ($P < .05$) as compared to untreated 2-copy control mice. The endogenous cGK activity of gene-duplicated 4-copy mice was increased by 2.8-fold as compared with 2-copy control mice (Figure 1A). Furthermore, renal cGK activity in 4-copy mice treated with A71915 and Rp was respectively reduced 45% ($P < .01$) and 32% ($P < .05$).

The protein levels of cGK I and cGK II in the kidneys of all the experimental animals were determined by Western blot analysis (Figure 1B). Densitometric analysis showed that cGK1 expression was reduced by 90% and cGK II expression by almost 66% in the kidneys of 0-copy mice as compared to 2-copy wild-type mice given the same treatments (Figure 1C,D). Gene-duplication of *Npr1* (4-copy) mice showed a significant increase in renal expression of cGK I (1.7-fold; $P < .01$) and cGK II (two-fold; $P < .001$).

There was a significant reduction in expression of cGK I (80%) and cGK II (67%) in 2-copy mice after A71915 treatment (Figure 1C,D). Similarly, after A71915 treatment for 15 days, 4-copy mice also showed significant compromises with renal cGK I (46%) and cGK II (65%) expression. Rp treatment led to reductions of only 20% in cGK I and 30% in cGK II expression in the kidneys of 4-copy mice compared with untreated control mice.

3.4 | Expression of MKP-1, cell-cycle regulators $p21^{Cip1}$/$p27^{Kip1}$, and MAPKs

We determined the expression of MKP-1, $p21^{Cip1}$, $p27^{Kip1}$, p-Erk1/2, and p-p38 to delineate the role of cGK-associated downstream targets in the development of hypertrophy in the kidneys of 2-copy and 4-copy mice given treatment with A71915 and Rp. The results demonstrated that administration of A71915 reduced the protective effect of GC-A/NPRA in the kidneys of 2-copy and 4-copy mice. A significant reduction in MKP-1 (70%) expression in 0-copy mice was observed as compared to that in 2-copy mice

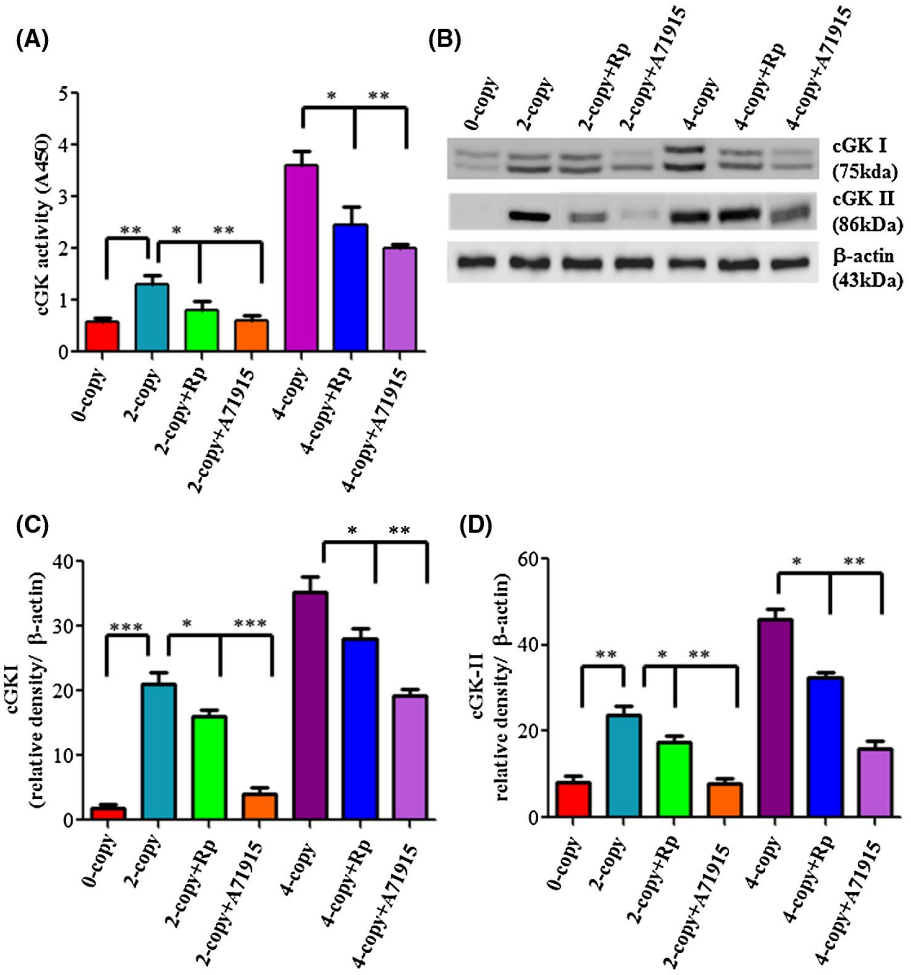

FIGURE 1 Comparative analysis of cGMP-dependent protein kinase activity and its renal expression in *Npr1* gene-disrupted, wild-type, and gene-duplicated mice with or without treatment of Rp-8-Br-cGMPS and A71915. A, cGK activity was measured according to the procedures as described in Materials and Methods section, in untreated 0-copy, 2-copy and 4-copy mice and 2-copy and 4-copy mice treated with Rp-8-Br-cGMPS and A71915 for 2 weeks. B, Shows the cGK I and cGK II protein expression by Western blot in the kidneys of the abovementioned groups. C and D, Respective densitometric quantitation of protein bands in Western blot analysis. The relative expression of cGK I and cGK II is compared with the relative expression of β-actin. Values are expressed as mean ± SE. $^{*}P < .05$; $^{**}P < .01$; $^{***}P < .001$, n = 10 mice in each group

(Figure 2A,B). After A71915 treatment for 15 days, the phosphorylation of MAPKs (p-Erk1/2 and p-p38) in 2-copy mice was significantly increased by 1.6-fold and 1.8-fold, respectively (Figure 2A,C,D). Simultaneously, there was a significant increase in expression levels of $p21^{Cip1}$ (1.7-fold) and $p27^{Kip1}$ (1.9-fold) in the kidneys of 2-copy mice after A71915 treatment (Figure 2A,E,F). Duplication of *Npr1* in 4-copy mice showed increased MKP-1 expression and attenuated levels of p-Erk1/2, p-p38, $p21^{Cip1}$, and $p27^{Kip1}$ as compared to levels in 2-copy mice (Figure 2A-F). Treatment with ANP antagonist, A71915, led to a greater reduction (50%; $P < .01$), while Rp treatment produced only partial attenuation (20%; $P < .05$) of MKP-1 expression in 4-copy mice. On the other hand, p-Erk1/2, p-p38, $p21^{Cip1}$, and $p27^{Kip1}$ expression levels were significantly increased in 4-copy mice after A71915 treatment as compared with levels in untreated control groups.

3.5 | Histochemical immunofluorescence analysis of PCNA, cGK I, cGK II, $p21^{Cip1}$, and $p27^{Kip1}$

To determine the immunofluorescence localization of PCNA, cGK I, cGK II, $p21^{Cip1}$, and $p27^{Kip1}$ under the inhibitor treatments, the kidney tissue sections were processed for immunofluorescence analysis with the specific antibodies of these proteins (Figure 3A-G). As shown in Table 2, there was a significant increase in renal PCNA expression in the kidneys of 0-copy (6.4-fold; Figure 3B) and 2-copy + A71915 (four-fold; Figure 3D) mice as compared with untreated 2-copy wild-type control mice (Figure 3A). Conversely, gene-duplication of *Npr1* in 4-copy mice showed a minimal, insignificant increases in the expression of PCNA after A71915 (Figure 3G) and Rp (Figure 3F) treatments. On the other hand, renal expression of cGK I

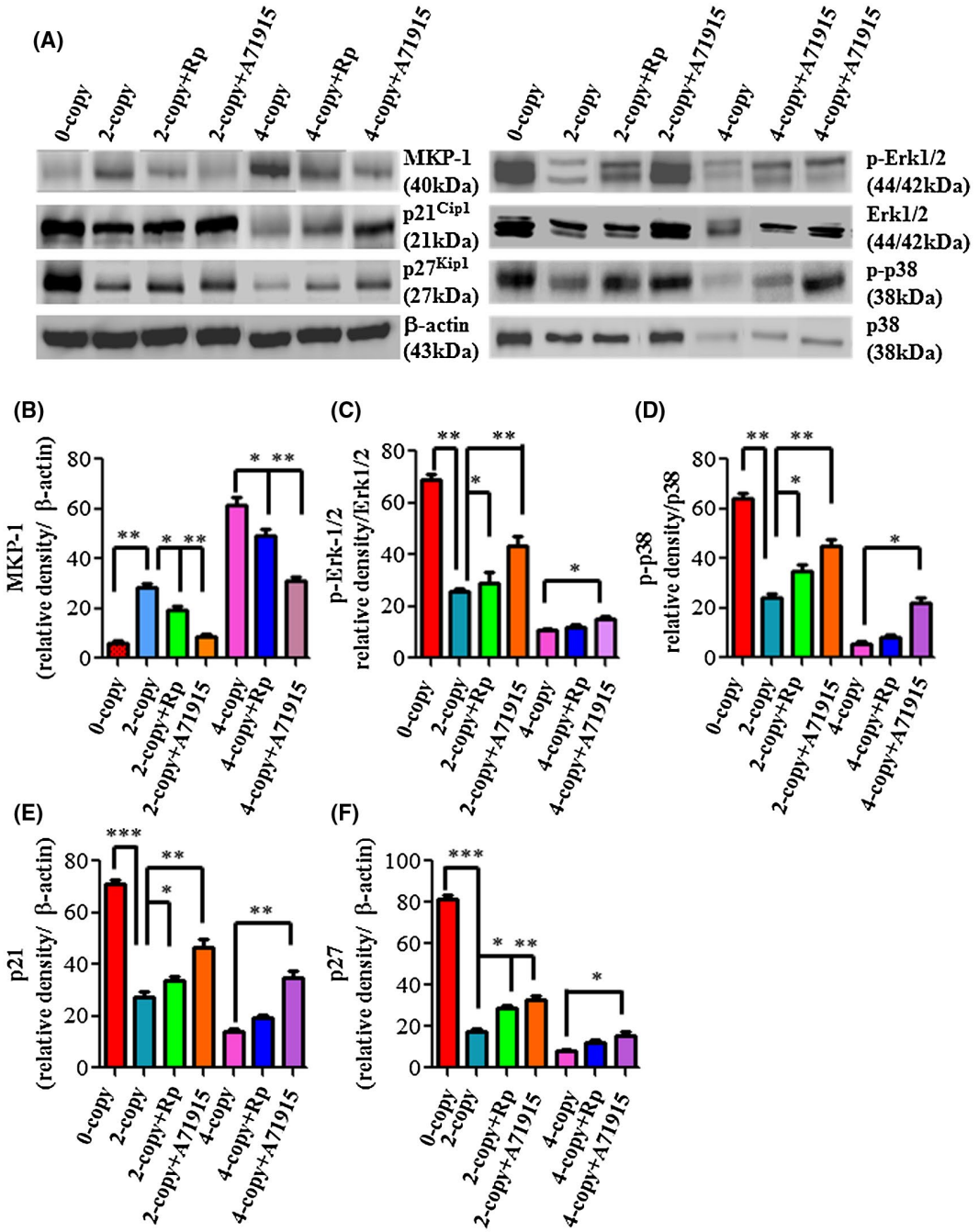

FIGURE 2 Quantitative analysis of renal expression of MKP-1, p-Erk1/2, p-p38 and cell-cycle modulatory protein molecules $p21^{Cip1}$ and $p27^{Kip1}$ in *Npr1* gene-disrupted, wild-type, and gene-duplicated mice with or without treatments of Rp-8-Br-cGMPS and A71915. A, The renal protein levels of MKP-1, p-Erk1/2, p-p38, $p21^{Cip1}$, and $p27^{Kip1}$ was determined by Western blot. B-F, Respective densitometric quantitation of protein bands in Western blot analysis. The relative expression of MKP-1, $p21^{Cip1}$, and $p27^{Kip1}$ is compared with the relative expression to β-actin. The relative expression of p-Erk1/2 and p-p38 MAPKs is compared with the relative expression Erk1/2 and p38, respectively. Values are expressed as mean ± SE. $^{*}P < .05$; $^{**}P < .01$; $^{***}P < .001$, n = 10 mice in each group

and cGK II was significantly reduced in 0-copy (Figure 3B) and 2-copy + A71915 (Figure 3D) mice but was only moderately altered in the 2-copy + Rp group (Figure 3C) as compared with 2-copy control mice (Table 2). *Npr1* gene-duplication in 4-copy mice led to significant increases in renal cGK I (1.8-fold) and cGK II (1.5-fold) expression as compared with that in wild-type 2-copy mice. Furthermore, treatment with both inhibitors produced modest but significant decreases in renal cGK I and cGK II expression in 4-copy mice given A71915 treatment (Table 2). The renal expression levels of $p21^{Cip1}$ and p^{27Kip1} in different groups of mice are shown in Figure 3A-G. The images

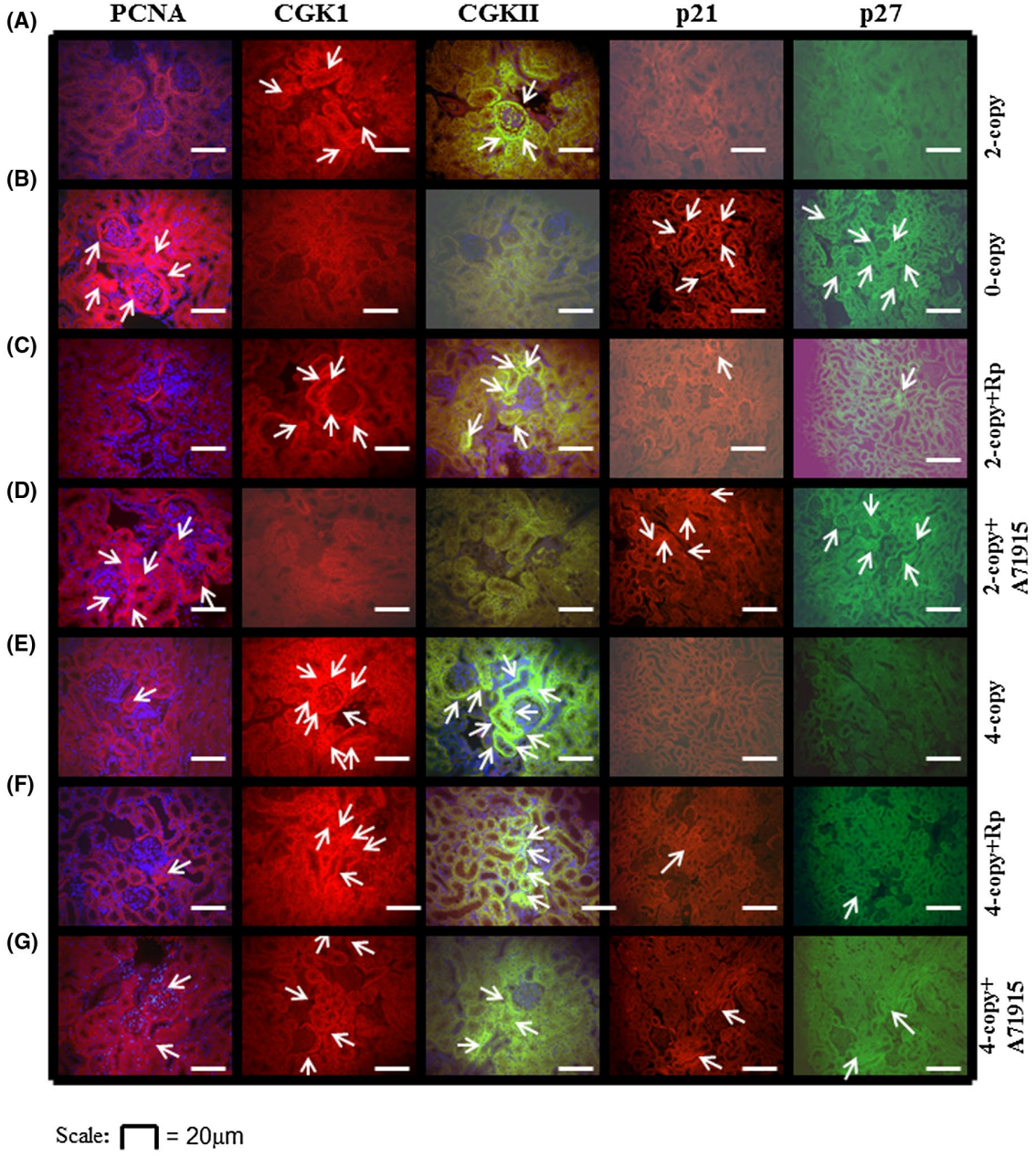

FIGURE 3 Histochemical immunofluorescence localization and expression of PCNA, cGK I, cGK II, $p21^{Cip1}$, and $p27^{Kip1}$ in the kidneys of *Npr1* gene-disrupted, wild-type and gene-duplicated mice. Kidney tissue section (4-μm) was used for the comparative analysis of the expression of PCNA, cGK I, cGK II, $p21^{Cip1}$, and $p27^{Kip1}$ according to the methods as described in the Materials and Methods section. A-G, Show representative images of 2-copy, 0-copy, 2-copy + Rp, 2-copy + A71915, 4-copy, 4-copy + Rp, and 4-copy + A71915 mice, respectively. Positive cells for each antibody are shown by white arrows in respective images. The images are representative of 10 mice in each group. Photomicrograph scale bar = 20 μm

shown here demonstrate a marked rise in renal expression of $p21^{Cip1}$ (nine-fold) and $p27^{Kip1}$ (seven-fold) in 2-copy mice after A71915 treatment; these expression levels were comparable to that in 0-copy mice (Figure 3B). However, A71915 and Rp treatment had little influence on $p21^{Cip1}$ and $p27^{Kip1}$ expression in the kidneys of 4-copy mice as compared to the respective untreated control animals (Figure 3E-G).

3.6 | Expression of mRNAs of cGK I, cGK II, and cytokines

We determined the mRNA expression levels of renal pro-inflammatory cytokines (TNF-α and IL-6), pro-fibrotic cytokine (TGF-β1), cGK I, and cGK II in *Npr1* mice given inhibitor treatments (Figure 4). Renal TNF-α mRNA expression was increased 9.4-fold in 0-copy mice as compared to

TABLE 2 Quantitative analysis of relative histochemical immunofluorescence localization of PCNA, cGK 1, cGK II, $p21^{Cip1}$ and $p27^{Kip1}$ in *Npr1* gene-disrupted, wild-type and gene-duplicated mice with or without Rp-8-Br-cGMPS (Rp) and A71915 treatments for 15 days

			2-copy			4-copy	
Parameters	**0-copy**	**2-copy**	**Rp**	**A71915**	**4-copy**	**Rp**	**A71915**
PCNA	51.3 ± 3.3[c]	8.0 ± 1.3	9.0 ± 1.3	32.6 ± 3.0[b]	4.2 ± 0.9	5.0 ± 0.6	7.0 ± 0.9
cGK 1	6.3 ± 0.9[c]	40.5 ± 2.6	32.8 ± 2.7[a]	9.4 ± 0.8[b]	70.9 ± 4.5	68.1 ± 3.9	55.3 ± 4.6[d]
cGK II	5.6 ± 0.9[c]	49.0 ± 4.0	38.5 ± 3.3[a]	7.4 ± 1.0[b]	82.6 ± 4.1	74.8 ± 5.0	67.1 ± 2.1 [d]
$p21^{Cip1}$	38.0 ± 3.2[c]	4.1 ± 0.9	5.4 ± 0.5	36.0 ± 2.2[b]	2.1 ± 0.9	3.2 ± 0.9	4.3 ± 0.6
$p27^{Kip1}$	44.2 ± 3.1[c]	5.1 ± 0.7	6.0 ± 0.9	35.8 ± 2.6[b]	2.4 ± 0.6	2.9 ± 0.7	3.7 ± 0.9

Note: Percentages for the antibody-positive area were calculated according to the method described under Materials and Methods section. The analysis was done for PCNA, proliferating cell nuclear antigen; cGK 1 and cGK II, cGMP-dependent protein kinase 1 and II; $p21^{Cip1}$ and $p27^{Kip1}$, cyclin dependent kinase (CDK) inhibitor protein. The antibody specificity was confirmed in the preliminary experiments using the PBS solution as a negative control in the absence of specific antibodies. Data are presented as mean ± SE. n = 8 in each group.

[a]$P < .05$ (untreated 2-copy vs Rp-treated wild-type, 2-copy).

[b]$P < .001$ (untreated 2-copy vs A71915-treated wild-type, 2-copy).

[c]$P < .001$ (untreated 2-copy vs untreated 0-copy).

[d]$P < .05$ (untreated gene-duplicated, 4-copy vs A71915-treated gene-duplicated, 4-copy).

2-copy control mice. A moderate increase in TNF-α mRNA was also observed in 2-copy mice treated with Rp, whereas a 6.6-fold increase occurred after treatment with A71915 (Figure 4A). Furthermore, TNF- α mRNA was moderately increased in 4-copy + A71915 mice (2.8-fold), but produced only small changes in 4-copy + Rp groups. Similarly, IL-6 mRNA was upregulated in 2-copy mice treated with Rp (3.2-fold; $P < .05$) and A71915 (7.2-fold; $P < .001$), the levels that were almost similar to those in 0-copy mice (10.3-fold; $P < .001$). Treatment of 4-copy mice with A71915 increased IL-6 mRNA by 2.7-fold ($P < .01$) as compared levels in untreated controls (Figure 4B). TGF-β1 mRNA was significantly increased in 2-copy (4.4-fold) and 4-copy (2.8-fold) mice treated with A71915 as compared with levels in their respective untreated controls (Figure 4C). Duplication of *Npr1* in 4-copy mice significantly increased the levels of cGK I mRNA (1.6-fold) and cGK II mRNA (2.3-fold) as compared to 2-copy control mice (Figure 4D,E). Conversely, deletion of *Npr1* from 0-copy mice reduced cGK I and cGK II mRNA levels by 80%-90%. Treatment with A71915 downregulated mRNA expression of cGK I and cGK II in 2-copy and 4-copy mice, whereas Rp treatment produced only minor changes in their mRNA expression as compared with untreated 2-copy control animals.

3.7 | Plasma and renal levels of cytokine proteins

The protein levels of TNF-α, IL-6, and TGF-β1 in both the plasma and kidneys of mice are shown in Figure 5. After A71915 treatment, the plasma TNF-α level was increased by 3.3-fold in 2-copy mice (8.3 ± 1.1 pg/mL (Figure 5A). Deletion of *Npr1* showed upregulation of plasma TNF-α level, by 6.5-fold in 0-copy mice as compared to the level in 2-copy control mice (16.17 ± 1.97 pg/mL vs 2.51 ± 0.63 pg/mL). Similarly, there was a 2.4-fold increase in the plasma TNF-α level in 4-copy mice after A71915 treatment. Kidney TNF-α concentration was also increased in 0-copy (two-fold), 2-copy + A71915 (1.7-fold), and 4-copy + A71915 (2.2-fold) mice as compared to their respective control mice (Figure 5D). After A71915 treatment, the IL-6 levels in both plasma and kidney were significantly increased in 2-copy (43.42 ± 2.08 pg/mL and 76.01 ± 3.37 pg/mg protein) and 4-copy mice (22.60 ± 1.86 pg/mL and 41.73 ± 2.48 pg/mg protein). However, Rp treatment led to only modest changes (Figure 5B,E). After treatment with A71915, plasma and kidney TGF-β1 levels were significantly increased in 0-copy mice (51.62 ± 5.22 pg/mL; three-fold and 167.7 ± 20.14 pg/mg protein; 4.2-fold), 2-copy mice (38.02 ± 1.81 pg/mL; 2.2-fold and 107.5 ± 5.56 pg/mg protein; 2.7-fold), and 4-copy mice (16.64 ± 3.18 pg/mL; 2.0-fold and 37.8 ± 2.42 pg/mg protein; 1.8-fold), respectively, (Figure 5C,F).

3.8 | Renal histopathology and morphometric analyses

Histological evaluation showed significantly marked increases in MME (indicated by black arrow), tubular hypertrophy (indicated by yellow arrow), tubulointerstitial nephritis (indicated by blue arrow), as well as perivascular infiltration of monocyte/macrophage (indicated by red arrow), in the kidney tissue sections of experimental mice (Figure 6A). MME, tubular hypertrophy, and tubulointerstitial nephritis, as well as perivascular infiltration (monocyte/macrophage), were seen in 0-copy, 2-copy + Rp, 2-copy + A71915, and 4-copy + A71915 mice as compared with untreated 2-copy

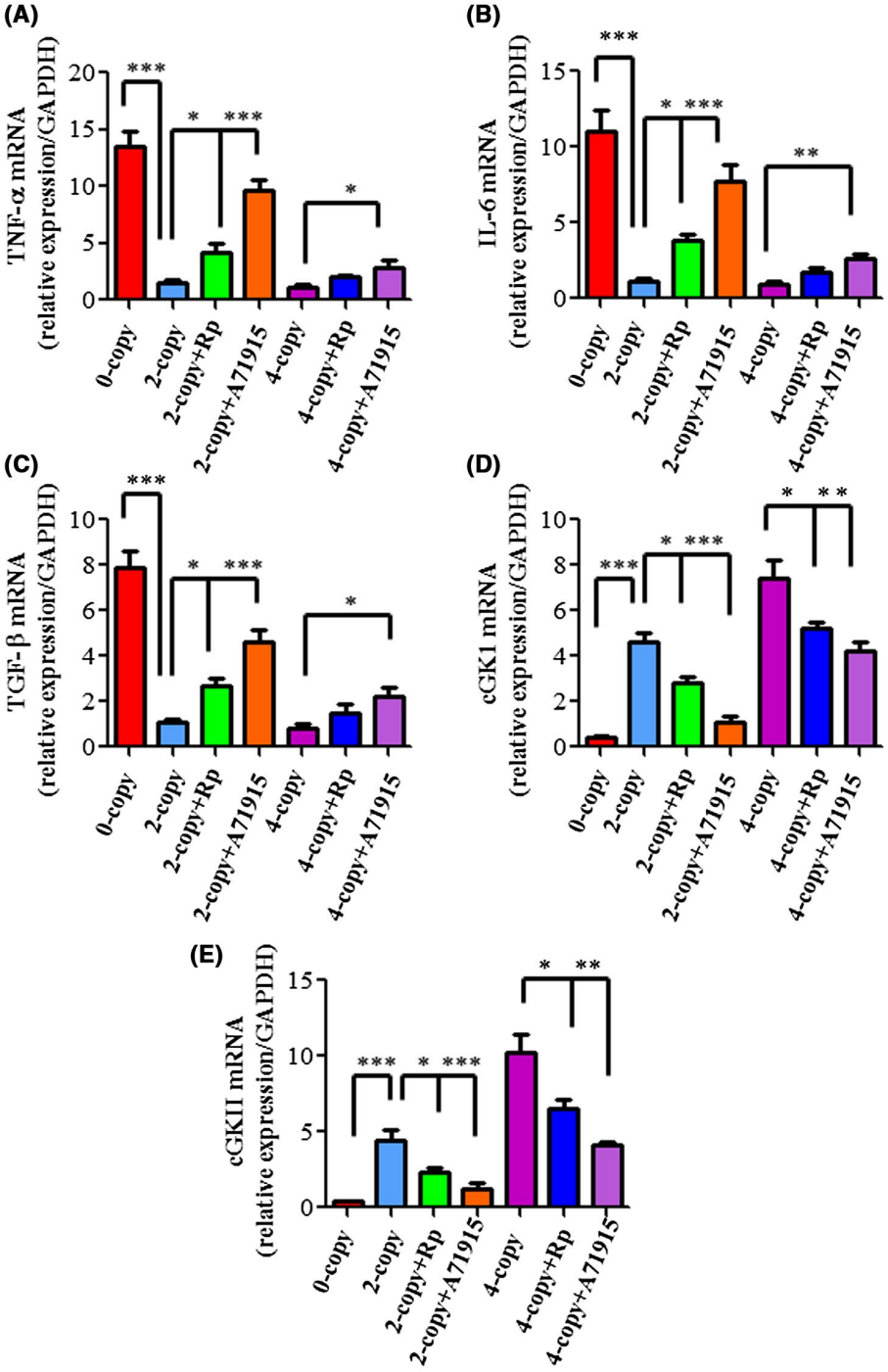

FIGURE 4 Renal pro-inflammatory cytokines, growth factor, and cGK genes in the kidney tissues of *Npr1* gene-disrupted, wild-type, and gene-duplicated mice. A and B, The relative mRNA expressions of pro-inflammatory cytokine, TNF-α and IL-6, normalized to GAPDH mRNA in the kidney tissues with or without inhibitor treatment. C, The mRNA expression of tissue growth factors and TGF-β1, relative to GAPDH mRNA in the kidney tissues. D and E, The relative mRNA expressions of cGK I and cGK II, respectively, in the kidney tissues relative to GAPDH. Values are expressed as mean ± SE. *$P < .05$; **$P < .01$; ***$P < .001$, n = 10 mice in each group

control mice. However, cellular integrity was only moderately changed in 4-copy mice after Rp treatments. The quantitative analyses of different renal pathologies in the tissue sections stained with H&E are presented in Figure 6C-F and Table 3. The quantitation of the data showed that the pathological incidence, including, MME, tubular hypertrophy, tubulointerstitial nephritis, and perivascular infiltration (monocyte/macrophage) was significantly higher in 0-copy mice and Rp- and A71915-treated 2-copy and 4-copy mice as compared to untreated control mice (Figure 6C-F; Table 3). However, the extent of damage was greater in 0-copy mice and A71915-treated 2-copy and 4-copy mice than untreated

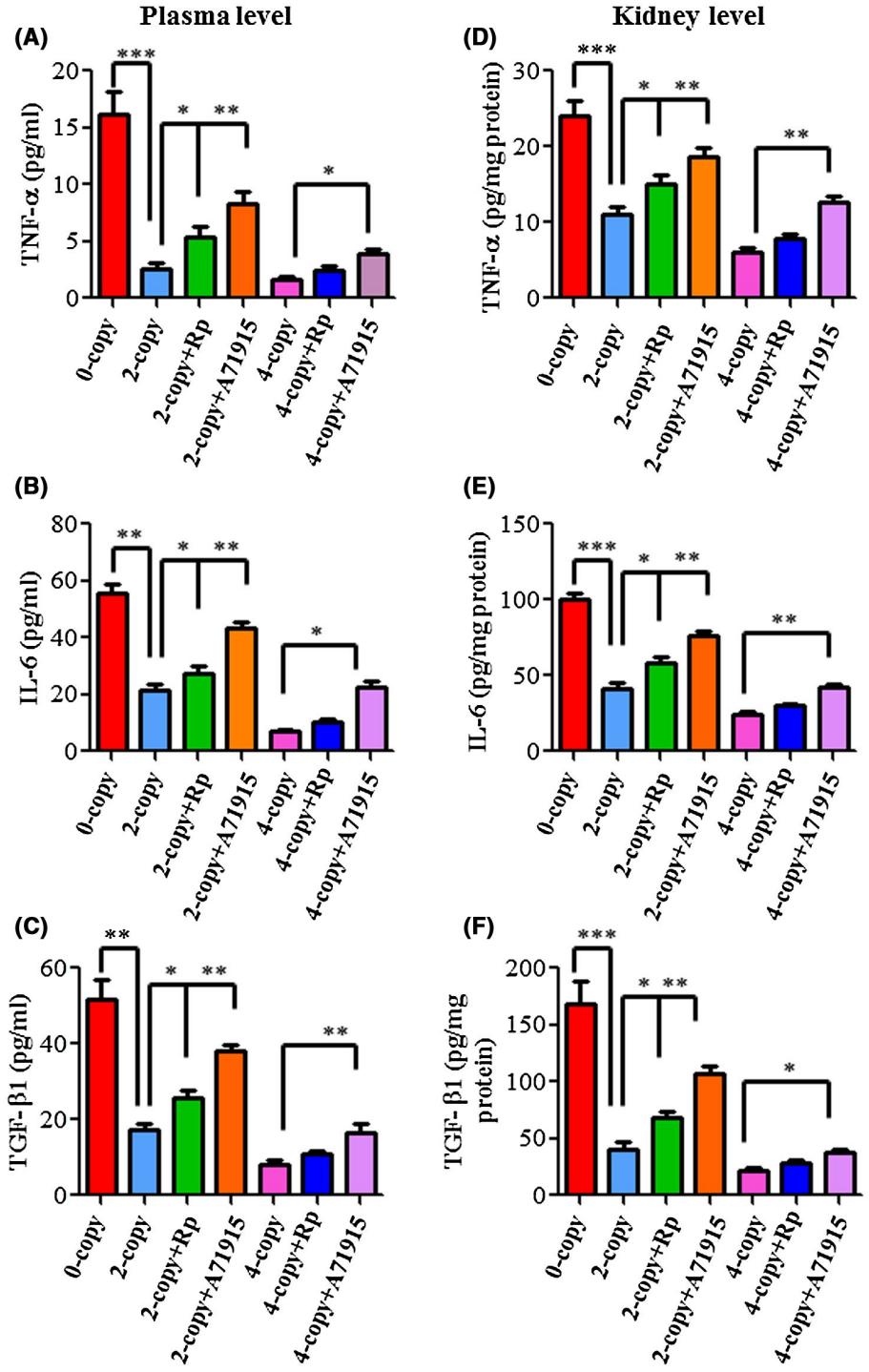

FIGURE 5 Quantitative analysis of plasma and kidney TNF-α, IL-6, and TGF-β1 in *Npr1* gene-disrupted, wild-type and gene-duplicated mice with or without treatment of Rp-8-br-cGMPS and A71915 inhibitors by multiplex assay. The concentrations of pro-inflammatory and pro-fibrotic cytokines were measured in plasma and kidney tissue homogenates by multiplex bead array format. A, B, and C, Plasma levels of TNF-α, IL-6, and TGF-β1. D, E, and F, Kidney levels of TNF-α, Il-6, and TGF-β1, respectively. Values are expressed as mean ± SE. $^{*}P < .05$; $^{**}P < .01$; $^{***}P < .001$, n = 10 mice in each group

control mice (Figure 6C-F). Renal fibrosis (shown by black arrows) was demonstrated in 0-copy mice by deposition of extracellular matrix (ECM), which is evident with the Masson's trichome blue staining of collagen fibers (Figure 6B). The treatments with A71915 yielded the similar deposition of collagen as observed in 0-copy mice; however, Rp-treated 2-copy and 4-copy mice showed mild blue coloration of kidney as compared with untreated control mice (Figure 6B). The quantitative analysis showed that the extent of fibrotic lesions was also greatly inflicted in 0-copy and A71915-treated 2-copy and 4-copy mice as compared with untreated control animals (Figure 6G; Table 3).

4 | DISCUSSION

Our results show that GC-A/NPRA has a pivotal role in anti-hypertrophic and anti-fibrotic responses through the stimulation of cGKs and attenuation of the CDK inhibitors $p21^{Cip1}$ and p^{27Kip1} in the kidneys of PKG inhibitor Rp-treated and NPRA antagonist, A71915-treated 2-copy and 4-copy mice. The data showed a significant 60% reduction in cGK

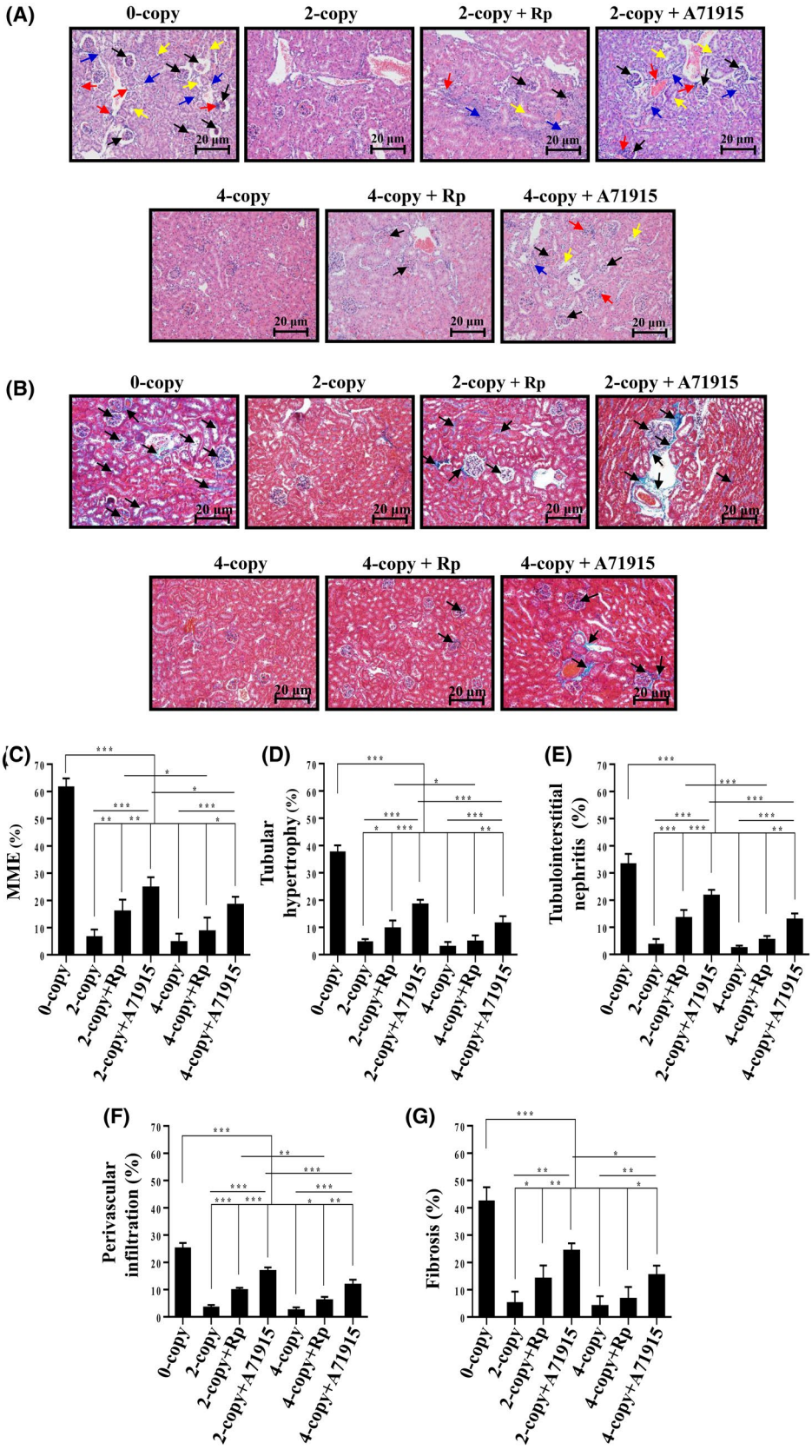

FIGURE 6 Analysis of renal histopathology of mesangial matrix expansion, tubular hypertrophy, tubulointerstitial nephritis, perivascular infiltration, and renal fibrosis in *Npr1* gene-disrupted, wild-type, and gene-duplicated mice. A, The kidney tissue sections stained with H&E show the histological evaluation with increased MME (indicated by black arrow), tubular hypertrophy (indicated by yellow arrow), tubulointerstitial nephritis (indicated by blue arrow), as well as perivascular infiltration of monocyte/macrophage (indicated in red arrow) in 0-copy, 2-copy + Rp, 2-copy + A71915, 4-copy + Rp, and 4-copy + A71915 mice as compared with untreated 2-copy control mice. B, The accumulation of collagen (fibrosis; blue-stained area) in the kidney sections of 0-copy, 2-copy + Rp, 2-copy + A71915, 4-copy + Rp, and 4-copy + A71915 mice, after staining with Masson's Trichrome (shown by black arrows). Panels C-F represent the quantitative analysis of MME, tubular hypertrophy, tubulointerstitial nephritis, and perivascular infiltration (monocyte/macrophage), respectively. Panel G represents the quantitative analysis of fibrosis. Photomicrograph scale bar = 20 μm. Veh, vehicle (saline)-treated group; *$P > .05$; **$P > .01$; ***$P > .001$; n = 8 mice in each group

activity in the kidneys of 0-copy mice and reductions of 53% and 45%, respectively, in the kidneys of NPRA antagonist-treated 2-copy and 4-copy mice. However, cGK activity was reduced by only 39% in Rp-treated 2-copy mice and 32% in Rp-treated 4-copy mice.

Earlier, cGK activity was shown to be modulated in many disease conditions, including diabetes and cancer.[59-61] Similarly, mRNA and protein levels of cGK-I were down-regulated in IR-induced kidney injury.[62] In the present study, gene-duplication in 4-copy mice showed a 2.7-fold increase in cGK activity, while both the NPRA antagonist and cGK inhibitor decreased its activity. cGK activity was reduced in 4-copy mice after treatment with A71915 (45%) and Rp (32%), but nevertheless failed to produce significant histological changes, probably because of the high residual basal cGK activity in these animals. We expected that the high basal cGK activity would remain elevated in the kidneys of 4-copy mice after the inhibitor treatments. Overexpression of cGK also attenuated IR-reperfusion-induced kidney injury in mice.[62] Moreover, there were significant decreases in protein expression of both cGK I and cGK II isozymes in the kidneys of 0-copy and 2-copy + A71915 mice, as well as a partial reduction in protein expression in 4-copy + A71915 mice. These decreases resulted in withdrawal of the counter-effective action of GC-A/NPRA against proliferative pathways, hypertrophy, and fibrosis in inhibitor-treated groups of mice. Similar results occurred in VSMCs, treated with high glucose.[63] On the other hand, *Npr1* gene-duplication led to an increase in protein levels of cGK I (1.7-fold) and cGK II (two-fold) in the kidneys of 4-copy mice. The high basal expression of cGK isozymes in the kidneys of 4-copy mice was confirmed by immunofluorescence analysis. Although treatment with the NPRA antagonist A71915 led to substantial reductions in both forms of cGK isoenzymes in 4-copy mice, Rp treatment did not produce significant changes, suggesting the superiority of treatment with A71915 rather than Rp. In the present studies, we observed two bands of cGK I and according to the molecular weight these might correspond with the isoenzymes cGK 1α and cGK Iβ; however, this needs further clarification. Interestingly, a previous report has indicated that ANP-dependent generation of cGMP activates cGK Iα that plays a critical role in the suppression of disease states.[24]

Previous studies, which showed that MAPKs (Erk1/2) are activated in diabetic nephropathy, also showed that blockade of MAPKs inhibited hypertrophy of mesangial cells.[30,64] The present study demonstrated a sharp rise in the phosphorylation of Erk1/2 and p38 MAPKs in 0-copy mice. Moreover, 2-copy and 4-copy mice treated with A71915 showed similar increases in p-Erk1/2 and p-p38 in the kidneys of these animals. The present findings are in agreement with our previous observations that ANP/NPRA system antagonized the agonist-stimulated MAPKs in VCSMs and MCs.[47,48] The toxic renal injury caused by experimental administration of mercuric chloride was found to be associated with the activation of renal MAPKs (Erk and JNK), which was further substantiated in the glycerol model of myoglobinuric acute renal injury.[65,66]

It has been suggested that the constitutive activation of Erk1/2 and p38 MAPKs plays an essential role in G_0-arrest of the cell cycle, which causes cellular hypertrophy.[67] It seems that activation of Erk1/2 and p38 is associated with the induction of cyclin D1, $p21^{Cip1}$, and p^{27Kip1} in the kidneys of *Npr1* 0-copy mice, as well as inhibitor-treated 2-copy and 4-copy mice. Previous studies have shown that, in contrast to cyclin D1, the induction of $p21^{Cip1}$ in the G1 phase of the cell cycle might be largely regulated by the magnitude, rather than the duration of activation of Erk1/2 and p38 MAPKs signals.[68-70] Thus, it seems that continuous and potent Erk1/2 and p38 activation should lead to the arrest of growth by long-term induction of $p21^{Cip1}$ and $p27^{Kip1}$. On the other hand, a biphasic but less potent Erk1/2 and p38 signal might primarily lead to cell proliferative and growth responsive signals.[68,70]

In agreement with those observations, our results suggest a simultaneous induction of $p21^{Cip1}$ and $p27^{Kip1}$ in the kidneys of 0-copy and A71915-treated 2-copy and 4-copy mice. Thus, sustained induction of CDK inhibitors $p21^{Cip1}$ and $p27^{Kip1}$ in 0-copy and A71915-treated 2-copy mice, as well as to a lesser extent in A71915-treated 4-copy mice, might halt cell transition and cause hypertrophy in the kidneys. Although higher levels of CGKs in 4-copy mice showed attenuated and limited induction of $p21^{Cip1}$ and $p27^{Kip1}$ in the kidneys, which seems to protect these animals from renal cell-cycle arrest, instead allows them to enter a normal cell-cycle transition.

The constitutive expression of MKP-1 attenuates the activation of MAPKs, thereby inhibiting cell proliferation.[45-48]

TABLE 3 Quantitative analysis of renal histopathological defects and percentage scoring for *Npr1* gene-disrupted, wild-type, and gene-duplicated mice with or without Rp-8-Br-cGMPS (Rp) and A71915 treatments for 15 days

			2-copy			4-copy	
Parameters	**0-copy**	**2-copy**	**Rp**	**A71915**	**4-copy**	**Rp**	**A71915**
MME	61.5 ± 3.3^{c}	6.5 ± 2.8	$15.8 \pm 4.5^{\#}$	24.6 ± 3.9^{b}	4.5 ± 3.3	8.5 ± 5.2	18.2 ± 3.1^{d}
Tubular hypertrophy	37.5 ± 2.6^{c}	4.5 ± 1.2	9.5 ± 3.0^{a}	18.2 ± 1.9^{b}	2.7 ± 1.9	4.6 ± 2.4	11.3 ± 2.8^{d}
Tubulointerstitial nephritis	33.2 ± 3.8^{c}	3.6 ± 2.1	$13.3 \pm 3.1^{\$}$	21.5 ± 2.3^{b}	2.2 ± 1.1	5.2 ± 1.6	12.7 ± 2.4^{d}
Perivascular infiltration	25.1 ± 2.0^{c}	3.4 ± 1.0	$9.6 \pm 1.0^{\$}$	16.6 ± 1.5^{b}	2.3 ± 1.2	5.9 ± 1.4	11.6 ± 2.0^{d}
Fibrosis	42.3 ± 5.2^{c}	5.1 ± 4.2	13.9 ± 5.0^{a}	$24.1 \pm 2.9^{¥}$	3.9 ± 3.7	6.5 ± 4.5	$15.2 \pm 3.6^{€}$

Note: Percentages for the renal defects were calculated according to the method described under Materials and Methods section. The renal histopathology scoring analysis was done for MME, tubular hypertrophy, tubulointerstitial nephritis, and perivascular infiltration. Data are presented as mean ± SE. n = 8 mice in each group.

[a]$P < .05$ (untreated 2-copy vs Rp-treated wild-type, 2-copy).

[b]$P < .001$ (untreated 2-copy vs A71915-treated wild-type, 2-copy).

[c]$P < .001$ (untreated 2-copy vs untreated 0-copy).

[d]$P < .001$ (untreated gene-duplicated, 4-copy vs A71915-treated gene-duplicated, 4-copy).

[#]$P < .01$ (untreated 2-copy vs Rp-treated wild-type, 2-copy).

[$]$P < .001$ (untreated 2-copy vs Rp-treated wild-type, 2-copy).

[¥]$P < .01$ (untreated 2-copy vs A71915-treated wild-type, 2-copy).

[€]$P < .01$ (untreated gene-duplicated, 4-copy vs A71915-treated gene-duplicated, 4-copy).

In this study, we found decreased MKP-1 expression in the absence of GC-A/NPRA signaling in the kidneys of 0-copy mice. Similarly, we observed that MKP-1 was downregulated in A71915-treated and Rp-treated 2-copy and 4-copy mice. However, gene-duplication of GC-A/NPRA enhanced the expression of MKP-1 in 4-copy mice. In contrast, p-Erk1/2 and p-p38 MAPKs were activated in 0-copy mice and also in the inhibitor-treated 2-copy and 4-copy mice. Similarly, the expression of pro-inflammatory cytokines was significantly greater in 0-copy mice and also in the inhibitor-treated 2-copy mice but to a lesser extent in 4-copy mice. These present results suggest that the increased expression of MKP-1 in the kidney in response to NPRA/cGMP signaling will antagonize the expression of pro-inflammatory molecules and will serve as a protective mechanism in the kidney. ANP has been shown to induce MKP-1 and inhibit MAPKs activation to block proliferation of mesangial cells.[47,48,71,72] Therefore, we propose that in the current study reduced MKP-1 expression exerted its withdrawal effect on dephosphorylation of Erk1/2 and p38 MAPKs and instead enhanced phosphorylation in untreated 0-copy mice, A71915- and Rp-treated 2-copy mice, and 4-copy mice. We have previously demonstrated that the ANP-NPRA system inhibits MAPKs, which seem to be critical for cell growth and proliferation.[48]

We observed diffuse interstitial and perivascular PCNA-positive cells in the kidneys of 0-copy mice and A71915-treated 2-copy and 4-copy mice. Such cells were present to a somewhat lesser extent in 4-copy mice, but in the untreated control groups there were only a few positive cells. Similarly, a few PCNA-positive cells were found in the renal tubular epithelium in the control groups but were abundant in 0-copy and A71915-treated 2-copy and 4-copy mice. Nevertheless, these cells were abundant in both the renal tubular epithelium and interstitial compartments. Earlier, we reported a simultaneous induction of cell proliferation and hypertrophy in the kidneys of *Npr1* gene-knockout mice.[10,11,13] Similar results have been reported in DOCA-salt-treated hypertensive rats.[73] The treatment of mice with A71915 caused an increase in PCNA-positive cells in the kidneys of 2-copy and 4-copy mice, indicating the role of MAPKs in cell proliferation and hypertrophic responses. In several previous studies, the activation of MAPKs has been reported in the regulation of cell growth, suggesting that they have essential roles in signal transduction leading to cell proliferation and hypertrophic growth responses.[74-77]

Our current finding shows increased levels of pro-inflammatory cytokines (TNF-α, IL-6) and pro-fibrotic cytokine (TGF-β1) in the plasma and kidneys of 0-copy and 2-copy + A71915 and 4-copy + A71915 mice. The increased levels of TNF-α, IL-6, and TGF-β1 appear to express the injured state of the kidney. Increased production of inflammatory cytokines has also been reported in IR kidneys in association with simultaneous increases in CDK-inhibitors $p21^{Cip1}$ and $p27^{Kip1}$.[78-80] In agreement with earlier findings, our present results demonstrate an increase in mRNA expression of TNF-α, IL-6, and TGFβ1 in the kidneys of 2-copy mice, as well as lesser increases in 4-copy mice after A71915 and Rp treatments. The expression levels of cytokines in inhibitor-treated 2-copy mice were significantly increased. However, these expression levels were only modestly increased in 4-copy mice as compared to untreated control mice.

Our present results suggest that overexpression of GC-A/NPRA may inhibit the transcription of cytokine genes more

strongly in 4-copy mice than in 2-copy mice. Earlier, we found that renal transcription of the pro-inflammatory cytokines was significantly increased in the absence of cGK/cGMP signaling in *Npr1* 0-copy mice.[5,11,13] We also showed that the depletion of cGMP was associated with increased mRNA expression of pro-inflammatory cytokine in 0-copy mice.[11,81] Similarly, the present results demonstrate depleted renal cGMP levels, which seem to be associated with decreased cGK protein expression and activity in the kidneys of *Npr1* 0-copy mice and 2-copy and 4-copy mice treated with Rp and A71915, leading to the renal hypertrophy, fibrosis, and renal dysfunction (Figure 7).

Previous studies have shown that cGMP directly regulates transcription factors by inducing phosphorylation or increasing the expression of short-lived proteins.[82-84] In the present study, we observed that despite the reduction of cGMP levels

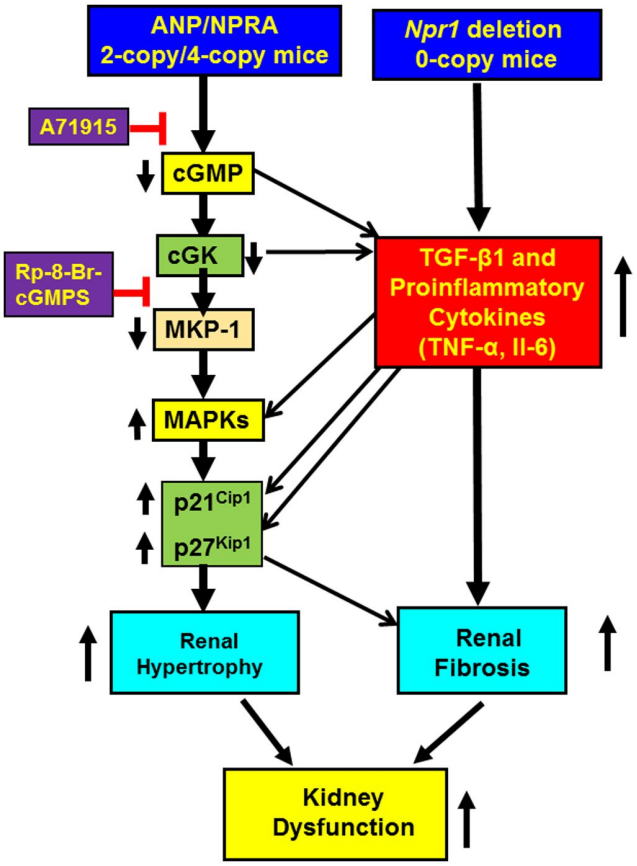

FIGURE 7 Proposed diagrammatic representation of ablated GC-A/NPRA signaling leading to renal hypertrophy and fibrosis. Deletion of GC-A/NPRA in 0-copy mice and treatments of 2-copy and 4-copy mice with A71915 and Rp-8-br-cGMPS, exhibited the depletion of cGMP/cGK levels, which in turn triggers the transcription and enhanced synthesis of pro-fibrotic cytokine (TGF-β1) and pro-inflammatory cytokines (TNF-α, IL-6) in the kidneys. The increased TGF-β1 level triggers increased induction and activation of MAPKs and/or CDK inhibitors $p21^{Cip1}$ and $p27^{Kip1}$ to produce renal hypertrophy and fibrosis in 0-copy mice and inhibitor-treated 2-copy and 4-copy mice

in both Rp inhibitor- and NPRA antagonist-treated 4-copy mice, the high residual levels of cGMP in these animals seem to be protective against possible renal injury inflicted by inhibitor treatments. In the present study, A71915 treatment induced significant increases in SBP in 2-copy mice, but only minimal increase in SBP in 4-copy mice. However, Rp treatment did not produce any significant changes in SBP in either 2-copy or 4-copy animals as compared with their respective controls. On the other hand, moderate and significant increases were found in KW, Alb:Cr ratio, and KC in A71915-treated 2-copy mice. There were only minor increases in 4-copy mice, but higher increases occurred in 0-copy mice without any inhibitor treatment.

The results of our study presented here suggest that progressive renal damage occurred in 0-copy, 2-copy + A71915, and 4-copy + A71915 mice. The pathological findings showed extensive development of MME and renal fibrosis in 0-copy and 2-copy + A71915 mice, perhaps as a result of increased SBP and reduced cGK/cGMP levels in these animals. Previously, we have shown the ED1 (CD68) immunostaining in the kidney for macrophage infiltration, which was at significantly higher levels in 0-copy mice than 2-copy mice.[10] In the present studies, we observed the infiltration of monocyte/macrophage using the histological evaluation, which indicated a significant higher levels of these inflammatory cells in 0-copy mice and also in the inhibitor-treated 2-copy and 4-copy animals. These present findings are in direct relationship with our previous reports, indicating that the significant infiltration of monocyte/macrophage contribute to the inflammatory molecules in the kidneys.[10,81] The absence of pathological findings, together with low SBP and higher basal cGK/cGMP levels in 2-copy + Rp, 4-copy + Rp,, and 4-copy + A71915 mice, confirmed the observation that low SBP and high cGK/cGMP levels have counter-regulatory effects against the incidence of renal hypertrophy and fibrosis in inhibitor-treated animals. Our results also suggest that gene-duplication of GC-A/NPRA has a greater protective effect against renal pathology MME in 4-copy mice under inhibitor treatment due to basal increased cGMP/cGK levels.

In summary, the present study has produced several important findings: (a) GC-A/NPRA has a crucial role in anti-hypertrophic and anti-fibrotic processes through the cGMP/cGK axis; (b) gene-duplication of *Npr1* induces increased levels of renal cGMP and enhanced expression of cGK, which attenuates renal pathology in 2-copy and 4-copy mice after treatment with NPRA-antagonist (A71915); (c) Rp treatment of 2-copy mice produced lesser differences in renal morphology and renal function than did A71915 treatment; (d) The inhibition of cGMP/cGK axis downregulates the phosphatase activity of MKP-1 and favors the phosphorylation of MAPKs, which triggers the induction of $p21^{Cip1}$ and $p27^{Kip1}$ to restrict the cells so that they remain in G_0 phase; (e) in turn, reduced cGMP/cGK levels trigger the expression of

pro-inflammatory (TNF-α, IL-6) and pro-fibrotic (TGF-β1) cytokine genes. The increased levels of TGF-β1 seem to induce cyclin and CDK inhibitors directly through MAPKs activation. Thereby, TGF-β1 and pro-inflammatory cytokines could then act as an amplifier to produce hypertrophy and fibrosis in the kidneys of 0-copy mice and NPRA antagonist-treated and to a lesser extent Rp-inhibitor-treated 2-copy and 4-copy mice.

ACKNOWLEDGMENTS

We thank Vickie Nguyen and Meagan Bloodworth for technical assistance and Kamala Pandey for assistance in the preparation of this manuscript. We are indebted to late Professor Oliver Smithies (University of North Carolina, Chapel Hill, NC) for providing the initial breeding pairs of *Npr1* gene-targeted mice colonies. This work was supported by a grant from the National Institutes of Health (HL 062147) and partial funds from the Tulane Carol Lavin Bernick grant award.

CONFLICT OF INTEREST

The authors declare no conflict of interest.

AUTHOR CONTRIBUTIONS

S. Das and K.N. Pandey designed the research: S. Das, K. Neelamegam, W.N. Peters, and R. Periyasamy performed the experiments: S. Das, K. Neelamegam, and K.N. Pandey analyzed the data: S. Das, K. Neelamegam, and K.N. Pandey wrote the manuscript.

REFERENCES

1. Oliver PM, Fox JE, Kim R, et al. Hypertension, cardiac hypertrophy, and sudden death in mice lacking natriuretic peptide receptor A. *Proc Natl Acad Sci USA*. 1997;94:14730-14735.
2. Pandey KN. Genetic ablation and guanylyl cyclase/natriuretic peptide receptor-A: impact on the pathophysiology of cardiovascular dysfunction. *Int J Mol Sci*. 2019;20(16):3946.
3. Epstein FH, Levin ER, Gardner DG, Samson WK. Natriuretic peptides. *N Engl J Med*. 1998;339:321-328.
4. Bryan PM, Xu X, Dickey DM, Chen Y, Potter LR. Renal hyporesponsiveness to atrial natriuretic peptide in congestive heart failure results from reduced atrial natriuretic peptide receptor concentrations. *Am J Physiol Renal Physiol*. 2007;292:F1636-1644.
5. Das S, Periyasamy R, Pandey KN. Activation of IKK/NF-kappaB provokes renal inflammatory responses in guanylyl cyclase/natriuretic peptide receptor-A gene-knockout mice. *Physiol Genomics*. 2012;44:430-442.
6. Prieto MC, Das S, Somanna NK, Harrison-Bernard LM, Navar LG, Pandey KN. Disruption of Npr1 gene differentially regulates the juxtaglomerular and distal tubular renin levels in null mutant mice. *Int J Physiol Pathophysiol Pharmacol*. 2012;4:128-139.
7. Shi SJ, Nguyen HT, Sharma GD, Navar LG, Pandey KN. Genetic disruption of atrial natriuretic peptide receptor-A alters renin and angiotensin II levels. *Am J Physiol Renal Physiol*. 2001;281:F665-673.
8. Zhao D, Das S, Pandey KN. Interactive roles of NPR1 gene-dosage and salt diets on cardiac angiotensin II, aldosterone and pro-inflammatory cytokines levels in mutant mice. *J Hypertens*. 2013;31:134-144.
9. Vellaichamy E, Zhao D, Somanna N, Pandey KN. Genetic disruption of guanylyl cyclase/natriuretic peptide receptor-A upregulates ACE and AT1 receptor gene expression and signaling: role in cardiac hypertrophy. *Physiol Genomics*. 2007;31:193-202.
10. Das S, Au E, Krazit ST, Pandey KN. Targeted disruption of guanylyl cyclase-A/natriuretic peptide receptor-A gene provokes renal fibrosis and remodeling in null mutant mice: role of proinflammatory cytokines. *Endocrinology*. 2010;151:5841-5850.
11. Kumar P, Gogulamudi VR, Periasamy R, Raghavaraju G, Subramanian U, Pandey KN. Inhibition of HDAC enhances STAT acetylation, blocks NF-kappaB, and suppresses the renal inflammation and fibrosis in Npr1 haplotype male mice. *Am J Physiol Renal Physiol*. 2017;313:F781-F795.
12. Nishikimi T, Inaba-Iemura C, Ishimura K, et al. Natriuretic peptide/natriuretic peptide receptor-A (NPR-A) system has inhibitory effects in renal fibrosis in mice. *Regul Pept*. 2009;154:44-53.
13. Periyasamy R, Das S, Pandey KN. Genetic disruption of guanylyl cyclase/natriuretic peptide receptor-A upregulates renal (pro) renin receptor expression in Npr1 null mutant mice. *Peptides*. 2019;114:17-28.
14. Sanches TR, Volpini RA, Massola Shimizu MH, et al. Sildenafil reduces polyuria in rats with lithium-induced NDI. *Am J Physiol Renal Physiol*. 2012;302:F216-225.
15. Tapia E, Sanchez-Lozada LG, Soto V, et al. Sildenafil treatment prevents glomerular hypertension and hyperfiltration in rats with renal ablation. *Kidney Blood Press Res*. 2012;35:273-280.
16. Airhart N, Yang YF, Roberts CT Jr, Silberbach M. Atrial natriuretic peptide induces natriuretic peptide receptor-cGMP-dependent protein kinase interaction. *J Biol Chem*. 2003;278:38693-38698.
17. Chang J, Zhang S, Wang N, et al. Enhanced performance of red perovskite light-emitting diodes through the dimensional tailoring of perovskite multiple quantum wells. *J Phys Chem Lett*. 2018;9:881-886.
18. Hofmann F, Wegener JW. cGMP-dependent protein kinases (cGK). *Methods Mol Biol*. 2013;1020:17-50.
19. Maimaitiyiming H, Li Y, Cui W, et al. Increasing cGMP-dependent protein kinase I activity attenuates cisplatin-induced kidney injury through protection of mitochondria function. *Am J Physiol Renal Physiol*. 2013;305:F881-890.
20. Wolfertstetter S, Reinders J, Schwede F, Ruth P, Schinner E, Schlossmann J. Interaction of cCMP with the cGK, cAK and MAPK kinases in murine tissues. *PLoS One*. 2015;10:e0126057.
21. Geiselhoringer A, Gaisa M, Hofmann F, Schlossmann J. Distribution of IRAG and cGKI-isoforms in murine tissues. *FEBS Lett*. 2004;575:19-22.
22. Joyce NC, DeCamilli P, Lohmann SM, Walter U. cGMP-dependent protein kinase is present in high concentrations in contractile cells of the kidney vasculature. *J Cyclic Nucleotide Protein Phosphor Res*. 1986;11:191-198.
23. Cui W, Maimaitiyiming H, Qi X, et al. Increasing cGMP-dependent protein kinase activity attenuates unilateral ureteral obstruction-induced renal fibrosis. *Am J Physiol Renal Physiol*. 2014;306:F996-1007.

24. Schinner E, Schramm A, Kees F, Hofmann F, Schlossmann J. The cyclic GMP-dependent protein kinase Ialpha suppresses kidney fibrosis. *Kidney Int*. 2013;84:1198-1206.
25. Schinner E, Wetzl V, Schramm A, et al. Inhibition of the TGFbeta signalling pathway by cGMP and cGMP-dependent kinase I in renal fibrosis. *FEBS Open Bio*. 2017;7:550-561.
26. Cheng X, Gao W, Dang Y, et al. Both ERK/MAPK and TGF-Beta/Smad signaling pathways play a role in the kidney fibrosis of diabetic mice accelerated by blood glucose fluctuation. *J Diabetes Res*. 2013;2013:463740.
27. Wang S, Wu X, Lincoln TM, Murphy-Ullrich JE. Expression of constitutively active cGMP-dependent protein kinase prevents glucose stimulation of thrombospondin 1 expression and TGF-beta activity. *Diabetes*. 2003;52:2144-2150.
28. Huang HC, Preisig PA. G1 kinases and transforming growth factor-beta signaling are associated with a growth pattern switch in diabetes-induced renal growth. *Kidney Int*. 2000;58:162-172.
29. Kuan CJ, Al-Douahji M, Shankland SJ. The cyclin kinase inhibitor p21WAF1, CIP1 is increased in experimental diabetic nephropathy: potential role in glomerular hypertrophy. *J Am Soc Nephrol*. 1998;9:986-993.
30. Wolf G, Sharma K, Chen Y, Ericksen M, Ziyadeh FN. High glucose-induced proliferation in mesangial cells is reversed by autocrine TGF-beta. *Kidney Int*. 1992;42:647-656.
31. Bretones G, Delgado MD, Leon J. Myc and cell cycle control. *Biochim Biophys Acta*. 2015;1849:506-516.
32. Lu Z, Hunter T. Ubiquitylation and proteasomal degradation of the p21(Cip1), p27(Kip1) and p57(Kip2) CDK inhibitors. *Cell Cycle*. 2010;9:2342-2352.
33. Wolf G, Schroeder R, Ziyadeh FN, Thaiss F, Zahner G, Stahl RA. High glucose stimulates expression of p27Kip1 in cultured mouse mesangial cells: relationship to hypertrophy. *Am J Physiol*. 1997;273:F348-356.
34. Zaidi ARS, Dresman S, Burt C, Rule S, McCallum L. Molecular signatures for CCN1, p21 and p27 in progressive mantle cell lymphoma. *J Cell Commun Signal*. 2019;13:421-434.
35. Al-Douahji M, Brugarolas J, Brown PA, Stehman-Breen CO, Alpers CE, Shankland SJ. The cyclin kinase inhibitor p21WAF1/CIP1 is required for glomerular hypertrophy in experimental diabetic nephropathy. *Kidney Int*. 1999;56:1691-1699.
36. Hannken T, Schroeder R, Zahner G, Stahl RA, Wolf G. Reactive oxygen species stimulate p44/42 mitogen-activated protein kinase and induce p27(Kip1): role in angiotensin II-mediated hypertrophy of proximal tubular cells. *J Am Soc Nephrol*. 2000;11:1387-1397.
37. Wolf G, Schroeder R, Thaiss F, Ziyadeh FN, Helmchen U, Stahl RA. Glomerular expression of p27Kip1 in diabetic db/db mouse: role of hyperglycemia. *Kidney Int*. 1998;53:869-879.
38. Wolf G, Schroeder R, Zahner G, Stahl RA, Shankland SJ. High glucose-induced hypertrophy of mesangial cells requires p27(Kip1), an inhibitor of cyclin-dependent kinases. *Am J Pathol*. 2001;158:1091-1100.
39. Cheng M, Sexl V, Sherr CJ, Roussel MF. Assembly of cyclin D-dependent kinase and titration of p27Kip1 regulated by mitogen-activated protein kinase kinase (MEK1). *Proc Natl Acad Sci*. 1998;95(3):1091-1096
40. Delmas C, Manenti S, Boudjelal A, Peyssonnaux C, Eychene A, Darbon JM. The p42/p44 mitogen-activated protein kinase activation triggers p27Kip1 degradation independently of CDK2/cyclin E in NIH 3T3 cells. *J Biol Chem*. 2001;276:34958-34965.
41. Kawada M, Yamagoe S, Murakami Y, Suzuki K, Mizuno S, Uehara Y. Induction of p27Kip1 degradation and anchorage independence by Ras through the MAP kinase signaling pathway. *Oncogene*. 1997;15:629-637.
42. Pumiglia KM, Decker SJ. Cell cycle arrest mediated by the MEK/mitogen-activated protein kinase pathway. *Proc Natl Acad Sci USA*. 1997;94:448-452.
43. Brondello JM, McKenzie FR, Sun H, Tonks NK, Pouyssegur J. Constitutive MAP kinase phosphatase (MKP-1) expression blocks G1 specific gene transcription and S-phase entry in fibroblasts. *Oncogene*. 1995;10:1895-1904.
44. Misra-Press A, Rim CS, Yao H, Roberson MS, Stork PJ. A novel mitogen-activated protein kinase phosphatase. Structure, expression, and regulation. *J Biol Chem*. 1995;270:14587-14596.
45. Noguchi T, Metz R, Chen L, Mattei MG, Carrasco D, Bravo R. Structure, mapping, and expression of erp, a growth factor-inducible gene encoding a nontransmembrane protein tyrosine phosphatase, and effect of ERP on cell growth. *Mol Cell Biol*. 1993;13:5195-5205.
46. Sun H, Tonks NK, Bar-Sagi D. Inhibition of Ras-induced DNA synthesis by expression of the phosphatase MKP-1. *Science*. 1994;266:285-288.
47. Sharma GD, Nguyen HT, Antonov AS, Gerrity RG, von Geldern T, Pandey KN. Expression of atrial natriuretic peptide receptor-A antagonizes the mitogen-activated protein kinases (Erk2 and P38MAPK) in cultured human vascular smooth muscle cells. *Mol Cell Biochem*. 2002;233:165-173.
48. Tripathi S, Pandey KN. Guanylyl cyclase/natriuretic peptide receptor-A signaling antagonizes the vascular endothelial growth factor-stimulated MAPKs and downstream effectors AP-1 and CREB in mouse mesangial cells. *Mol Cell Biochem*. 2012;368:47-59.
49. Pandey KN, Oliver PM, Maeda N, Smithies O. Hypertension associated with decreased testosterone levels in natriuretic peptide receptor-A gene-knockout and gene-duplicated mutant mouse models. *Endocrinology*. 1999;140:5112-5119.
50. Smithies O, Kim HS. Targeted gene duplication and disruption for analyzing quantitative genetic traits in mice. *Proc Natl Acad Sci USA*. 1994;91:3612-3615.
51. Oliver PM, John SW, Purdy KE, et al. Natriuretic peptide receptor 1 expression influences blood pressures of mice in a dose-dependent manner. *Proc Natl Acad Sci USA*. 1998;95:2547-2551.
52. Shi SJ, Vellaichamy E, Chin SY, Smithies O, Navar LG, Pandey KN. Natriuretic peptide receptor A mediates renal sodium excretory responses to blood volume expansion. *Am J Physiol Renal Physiol*. 2003;285:F694-702.
53. Vellaichamy E, Khurana ML, Fink J, Pandey KN. Involvement of the NF-kappa B/matrix metalloproteinase pathway in cardiac fibrosis of mice lacking guanylyl cyclase/natriuretic peptide receptor A. *J Biol Chem*. 2005;280:19230-19242.
54. Vellaichamy E, Das S, Subramanian U, Maeda N, Pandey KN. Genetically altered mutant mouse models of guanylyl cyclase/natriuretic peptide receptor-A exhibit the cardiac expression of proinflammatory mediators in a gene-dose-dependent manner. *Endocrinology*. 2014;155:1045-1056.
55. Wang JJ, Zhang SX, Mott R, et al. Salutary effect of pigment epithelium-derived factor in diabetic nephropathy: evidence for antifibrogenic activities. *Diabetes*. 2006;55:1678-1685.
56. Jamall IS, Finelli VN, Que Hee SS. A simple method to determine nanogram levels of 4-hydroxyproline in biological tissues. *Anal Biochem*. 1981;112:70-75.

57. Somanna NK, Pandey AC, Arise KK, Nguyen V, Pandey KN. Functional silencing of guanylyl cyclase/natriuretic peptide receptor-A by microRNA interference: analysis of receptor endocytosis. *Int J Biochem Mol Biol*. 2013;4:41-53.
58. Hesabi B, Danziger RS, Kotlo KU. Heterogeneous nuclear ribonucleoprotein A1 is a novel cellular target of atrial natriuretic peptide signaling in renal epithelial cells. *Cell Signal*. 2012;24:1100-1108.
59. Chang S, Hypolite JA, Velez M, et al. Downregulation of cGMP-dependent protein kinase-1 activity in the corpus cavernosum smooth muscle of diabetic rabbits. *Am J Physiol Regul Integr Comp Physiol*. 2004;287:R950-R960.
60. Deguchi A, Thompson WJ, Weinstein IB. Activation of protein kinase G is sufficient to induce apoptosis and inhibit cell migration in colon cancer cells. *Cancer Res*. 2004;64:3966-3973.
61. Jacob A, Smolenski A, Lohmann SM, Begum N. MKP-1 expression and stabilization and cGK Ialpha prevent diabetes- associated abnormalities in VSMC migration. *Am J Physiol Cell Physiol*. 2004;287:C1077-1086.
62. Li Y, Tong X, Maimaitiyiming H, Clemons K, Cao JM, Wang S. Overexpression of cGMP-dependent protein kinase I (PKG-I) attenuates ischemia-reperfusion-induced kidney injury. *Am J Physiol Renal Physiol*. 2012;302:F561-570.
63. Liu S, Ma X, Gong M, Shi L, Lincoln T, Wang S. Glucose down-regulation of cGMP-dependent protein kinase I expression in vascular smooth muscle cells involves NAD(P)H oxidase-derived reactive oxygen species. *Free Radic Biol Med*. 2007;42:852-863.
64. Ernest S, Bello-Reuss E. Xenobiotic transport differences in mouse mesangial cell clones expressing mdr1 and mdr3. *Am J Physiol*. 1996;270:C910-C919.
65. Ishizuka S, Yano T, Hagiwara K, et al. Extracellular signal-regulated kinase mediates renal regeneration in rats with myoglobinuric acute renal injury. *Biochem Biophys Res Commun*. 1999;254:88-92.
66. Yano T, Yano Y, Yuasa M, et al. The repetitive activation of extracellular signal-regulated kinase is required for renal regeneration in rat. *Life Sci*. 1998;62:2341-2347.
67. Roovers K, Assoian RK. Integrating the MAP kinase signal into the G1 phase cell cycle machinery. *BioEssays*. 2000;22:818-826.
68. Sebolt-Leopold JS, Dudley DT, Herrera R, et al. Blockade of the MAP kinase pathway suppresses growth of colon tumors in vivo. *Nat Med*. 1999;5:810-816.
69. Chang TS, Kim MJ, Ryoo K, et al. p57KIP2 modulates stress-activated signaling by inhibiting c-Jun NH2-terminal kinase/stress-activated protein Kinase. *J Biol Chem*. 2003;278:48092-48098.
70. Huang S, Shu L, Dilling MB, et al. Sustained activation of the JNK cascade and rapamycin-induced apoptosis are suppressed by p53/p21(Cip1). *Mol Cell*. 2003;11:1491-1501.
71. Kiemer AK, Weber NC, Furst R, Bildner N, Kulhanek-Heinze S, Vollmar AM. Inhibition of p38 MAPK activation via induction of MKP-1: atrial natriuretic peptide reduces TNF-alpha-induced actin polymerization and endothelial permeability. *Circ Res*. 2002;90:874-881.
72. Sugimoto T, Haneda M, Togawa M, et al. Atrial natriuretic peptide induces the expression of MKP-1, a mitogen-activated protein kinase phosphatase, in glomerular mesangial cells. *J Biol Chem*. 1996;271:544-547.
73. Peng H, Carretero OA, Alfie ME, Masura JA, Rhaleb NE. Effects of angiotensin-converting enzyme inhibitor and angiotensin type 1 receptor antagonist in deoxycorticosterone acetate-salt hypertensive mice lacking Ren-2 gene. *Hypertension*. 2001;37:974-980.
74. Karin M. The regulation of AP-1 activity by mitogen-activated protein kinases. *J Biol Chem*. 1995;270:16483-16486.
75. Marshall CJ. Specificity of receptor tyrosine kinase signaling: transient versus sustained extracellular signal-regulated kinase activation. *Cell*. 1995;80:179-185.
76. Seger R, Krebs EG. The MAPK signaling cascade. *FASEB J*. 1995;9:726-735.
77. Besson A, Dowdy SF, Roberts JM. CDK inhibitors: cell cycle regulators and beyond. *Dev Cell*. 2008;14:159-169.
78. Browner NC, Sellak H, Lincoln TM. Downregulation of cGMP-dependent protein kinase expression by inflammatory cytokines in vascular smooth muscle cells. *Am J Physiol Cell Physiol*. 2004;287:C88-96.
79. Monkawa T, Hiromura K, Wolf G, Shankland SJ. The hypertrophic effect of transforming growth factor-beta is reduced in the absence of cyclin-dependent kinase-inhibitors p21 and p27. *J Am Soc Nephrol*. 2002;13:1172-1178.
80. Mortensen J, Shames B, Johnson CP, Nilakantan V. MnTMPyP, a superoxide dismutase/catalase mimetic, decreases inflammatory indices in ischemic acute kidney injury. *Inflamm Res*. 2011;60:299-307.
81. Gogulamudi VR, Mani I, Subramanian U, Pandey KN. Genetic disruption of Npr1 depletes regulatory T cells and provokes high levels of proinflammatory cytokines and fibrosis in the kidneys of female mutant mice. *Am J Physiol Renal Physiol*. 2019;316:F1254-F1272.
82. Casteel DE, Zhuang S, Gudi T, et al. cGMP-dependent protein kinase I beta physically and functionally interacts with the transcriptional regulator TFII-I. *J Biol Chem*. 2002;277:32003-32014.
83. Gudi T, Chen JC, Casteel DE, Seasholtz TM, Boss GR, Pilz RB. cGMP-dependent protein kinase inhibits serum-response element-dependent transcription by inhibiting rho activation and functions. *J Biol Chem*. 2002;277:37382-37393.
84. Sauzeau V, Rolli-Derkinderen M, Marionneau C, Loirand G, Pacaud P. RhoA expression is controlled by nitric oxide through cGMP-dependent protein kinase activation. *J Biol Chem*. 2003;278:9472-9480.

How to cite this article: Das S, Neelamegam K, Peters WN, Periyasamy R, Pandey KN. Depletion of cyclic-GMP levels and inhibition of cGMP-dependent protein kinase activate $p21^{Cip1}$/$p27^{Kip1}$ pathways and lead to renal fibrosis and dysfunction. *The FASEB Journal*. 2020;34:11925–11943. https://doi.org/10.1096/fj.202000754R